Title	Glycomics microarrays reveal differential in situ presentation of the biofilm polysaccharide Poly-N-acetylglucosamine on Acinetobacter baumannii and Staphylococcus aureus cell surfaces
Author(s)	Flannery, Andrea; Le Berre, Marie; Pier, Gerald B.; O'Gara, James P.; Kilcoyne, Michelle
Publication Date	2020-04-02
Publication Information	Flannery, Andrea, Le Berre, Marie, Pier, Gerald B., O'Gara, James P., & Kilcoyne, Michelle. (2020). Glycomics Microarrays Reveal Differential In Situ Presentation of the Biofilm Polysaccharide Poly-N-acetylglucosamine on Acinetobacter baumannii and Staphylococcus aureus Cell Surfaces. 21(7), 2465, doi:10.3390/ijms21072465
Publisher	MDPI
Link to publisher's version	https://doi.org/10.3390/ijms21072465
Item record	http://hdl.handle.net/10379/15868
DOI	http://dx.doi.org/10.3390/ijms21072465

Glycomics microarrays reveal differential *in situ* presentation of the biofilm polysaccharide poly-*N*-acetylglucosamine on *Acinetobacter baumannii* and *Staphylococcus aureus* cell surfaces

Andrea Flannery,[1,2] Marie Le Berre,[3] Gerald B. Pier,[4] James P. O'Gara,[2] Michelle Kilcoyne[1,3,*]

[1] Carbohydrate Signalling Group, Discipline of Microbiology, National University of Ireland Galway, Galway, Ireland.

[2] Infectious Disease Laboratory, Discipline of Microbiology, National University of Ireland Galway, Galway, Ireland.

[3] Advanced Glycoscience Research Cluster, School of Natural Sciences, National University of Ireland Galway, Galway, Ireland.

[4] Division of Infectious Diseases, Department of Medicine, Brigham and Women's Hospital, Harvard Medical School, Boston, MA, U.S.A.

***** Corresponding author. Email: Michelle.Kilcoyne@nuigalway.ie

Keywords: Biofilm, glycomics microarrays, bacterial adhesins, polysaccharide, *Staphylococcus aureus*, *Acinetobacter baumannii*, poly-*N*-acetylglucosamine, PNAG, lectin

Abstract

The biofilm component poly-*N*-acetylglucosamine (PNAG) is an important virulence determinant in medical device-related infections caused by ESKAPE group pathogens including Gram-positive *Staphylococcus aureus* and Gram-negative *Acinetobacter baumannii*. PNAG presentation on bacterial cell surfaces and its accessibility for host interactions are not fully understood. We employed a lectin microarray to examine PNAG surface presentation and interactions on methicillin-sensitive (MSSA) and methicillin-resistant *S. aureus* (MRSA) and a clinical *A. baumannii* isolate. Purified PNAG bound to wheatgerm agglutinin (WGA) and succinylated WGA (sWGA) lectins only. PNAG was the main accessible components on MSSA but was relatively inaccessible on the *A. baumannii* surface, where it modulated the presentation of other surface molecules. Carbohydrate microarrays demonstrated similar specificities of *S. aureus* and *A. baumannii* for their most intensely binding carbohydrates, including 3' and 6'sialyllactose, but differences in moderately binding ligands, including blood groups A and B. An *N*-acetylglucosamine-binding lectin function on the *A. baumannii* cell surface which binds to PNAG was identified, which we hypothesise contributes to biofilm structure and PNAG surface presentation on *A. baumannii*. These data indicated differences in PNAG presentation and accessibility for interactions on Gram-positive and Gram-negative cell surfaces which may play an important role in biofilm-mediated pathogenesis.

INTRODUCTION

Biofilms are formed by bacteria to adapt to environmental changes and protect themselves from the host immune system and other environments. Composed of microbial cells, exopolysaccharides, extracellular DNA (eDNA) and proteins, biofilms account for over 80% of microbial infections in humans [1] and are a major cause of hospital-acquired infections, notably associated with medical device infections [2]. In Europe, these infections resulted in 16 million extra days in hospital between 1995 and 2010, costing €7 billion and 37,000 deaths, while in the USA in the same period, 1.7 million patients acquired an infection in hospitals and 99,000 died from these infections [3]. Gram-positive *Staphylococcus aureus* and Gram-negative *Acinetobacter baumannii* are leading causes of hospital-acquired biofilm infections and members of the antibiotic-resistant 'ESKAPE' group of pathogens [4]. Both *S. aureus* and *A. baumannii* produce poly-*N*-acetylglucosamine (PNAG, Figure 1(a)) as a major component of their biofilm matrix, as well as retaining PNAG on their cell surfaces. PNAG plays a fundamental role in the adhesion of *S. aureus* and *A. baumannii* cells within the biofilm matrix and has been implicated as a virulence factor important for *S. aureus* pathogenesis [5,6]. In contrast, there has been no correlation between PNAG production and *A. baumannii* virulence to date [7]. Correlations have been made between *S. aureus* antibiotic susceptibility and PNAG production, and antibiotic susceptibility and biofilm formation in *A. baumannii* [7-9]. However, the presentation of PNAG *in situ* on the bacterial cell surface, PNAG interaction(s) and recognition by the host's innate immune system and the consequential effects on the immune system are still uncertain [5,10]. A better understanding of the presentation and accessibility of this important biofilm component on the bacterial cell surface could help to shed light on host-pathogen interactions and mechanisms of antimicrobial resistance and immune evasion.

Biofilms can be regarded as dynamic and responsive to the environment and PNAG expression is influenced by a range of environmental factors including the availability of glucose, urea, and ethanol [11-13]. To our knowledge, it is not known whether altered growth conditions cause alterations in PNAG presentation on the bacterial surface or variations in the interactions of PNAG, although differences in surface glycosylation have been noted by lectin agglutination assays for methicillin-resistant *S. aureus* (MRSA) clinical strains under different culture conditions [14]. It is challenging to characterise and analyse biofilm and biofilm components, and laser microscopy in combination with fluorescently labelled lectins is one of the most common methods currently used to characterise biofilm carbohydrate and

glycoconjugate content [15]. However, this method does not lend itself well to high throughput or multi-omics strategies, in particular glycomics which is important for understanding host-pathogen interactions [16].

In addition to exopolysaccharides, secreted extracellular proteins, cell surface adhesins and protein subunits of flagella and pili participate in biofilm assembly and some of these bacterial proteins have lectin function [17]. Recently, the outer membrane-bound *P. aeruginosa* lectin, LecB (or PA-IIL), was shown to bind to the secreted biofilm exopolysaccharide Psl and thereby tether the bacterium to the biofilm matrix and facilitate biofilm assembly [18]. To date, only limited carbohydrate binding specificities have been characterised for *S. aureus* or *A. baumannii*, but to the best of our knowledge, there has been no investigation of the role of bacterial surface lectins in *S. aureus* or *A. baumannii* binding to biofilm component polysaccharides or in biofilm assembly or presentation.

Lectin microarrays have been used for profiling bacterial surface glycosylation [19-21] while carbohydrate microarrays have been used to characterise the structural specificity of bacterial interactions [22]. However, glycomic microarrays have not been used to examine the presentation or interactions of intact biofilm components *in situ* on the bacterial cell surface, bacterial surface lectins potentially involved in biofilm assembly, or any potential influence of biofilm components on the presentation of other bacterial surface molecules. In this work, we describe the use of a lectin microarray to examine the *in situ* presentation of PNAG on the cell surface of methicillin-sensitive *S. aureus* (MSSA) and methicillin-resistent *S. aureus* (MRSA) strains and *A. baumannii*. The plant lectins wheatgerm agglutinin (WGA) and succinylated WGA (sWGA) were the only lectins to bind to PNAG alone from a panel of 48 lectins assessed. We observed differential surface presentation of PNAG between the Gram-positive and Gram-negative species, and differences in accessibility of PNAG for interactions with lectins. Further, carbohydrate microarrays identified the carbohydrate binding specificity of all strains in this study and revealed a role for a surface lectin function in biofilm assembly for *A. baumannii*. This approach contributes to the glycomics of multi-omics strategies for understanding host-pathogen interactions [16] and could provide a high-throughput method for rapidly studying biofilm components *in situ* on the cell surface.

RESULTS AND DISCUSSION

Bacterial strains selection and verification of biofilm production. The MSSA strains 8325-4 and Mn8m were selected as Gram-positive organisms that produce PNAG-

predominant biofilm (Table 1 and Table S1) [23,24]. In *S. aureus*, PNAG is produced by proteins encoded in the *ica* operon and thus the Δ*ica* mutants of the *S. aureus* strains [25,26] were included in this study. The MRSA clinical isolate strain BH1CC has an *ica* operon but does not produce PNAG. Instead eDNA is the main biofilm component [27]. *S. aureus* BH1CC wild type (WT) and the Δ*ica* mutant were included for comparison with the MSSA strains. In some species of Gram-negative bacteria, PNAG is synthesised by proteins produced by the *pga* operon, so the PNAG-producing clinical isolate *A. baumannii* strain S1 WT and its Δ*pga* mutant [28] were also included. Anti-PNAG monoclonal antibody (mAb) was used in a dot blot assay to confirm that the PNAG-producing strains *S. aureus* 8325-4, *S. aureus* Mn8m and *A. baumannii* S1 cultured under biofilm-promoting conditions retained PNAG *in situ* on the cell surface under experimental conditions, while the Δ*ica* and Δ*pga* mutants did not produce any PNAG as expected (Figure 1(b)).

Crystal violet biofilm assays confirmed that *S. aureus* strains 8325-4 and Mn8m WT had increased biofilm formation in the presence of glucose and/or NaCl and that this biofilm was primarily composed of PNAG. *S. aureus* BH1CC WT had increased biofilm formation in the presence of glucose and decreased or abolished biofilm in NaCl. PNAG was not involved in *S. aureus* BH1CC biofilm formation, as expected, and PNAG contributed to *A. baumannii* S1 biofilm formation (Table 1 and Figure S1).

Table 1. Major biofilm type and effects of glucose and NaCl on biofilm formation by selected bacterial strains. All reports for *S. aureus* are based on biofilm assays carried out on hydrophilic 96-well plates [9,25-27,29-31]. Reports for *A. baumannii* are based on biofilm formation on borosilicate glass tubes [28]. n.d. – not determined in reports to date. n.a. – not applicable.

Species and strain	**Sensitivity**	**Additive**	**Biofilm effect**	**Major biofilm type**		
				Protein	**eDNA**	**PNAG**
S. aureus 8325-4	MSSA	Glc	↑			✓
		NaCl	↑			✓
S. aureus Mn8m	MSSA	Glc	↑			✓
		NaCl	n.d.	n.d.	n.d.	n.d.
S. aureus BH1CC	MRSA	Glc	↑	✓	✓	
		NaCl	↓	n.d.	n.d.	n.d.
A. baumannii S1	n.d.	Glc	n.d.			✓
		NaCl	n.d.	n.d.	n.d.	n.d.

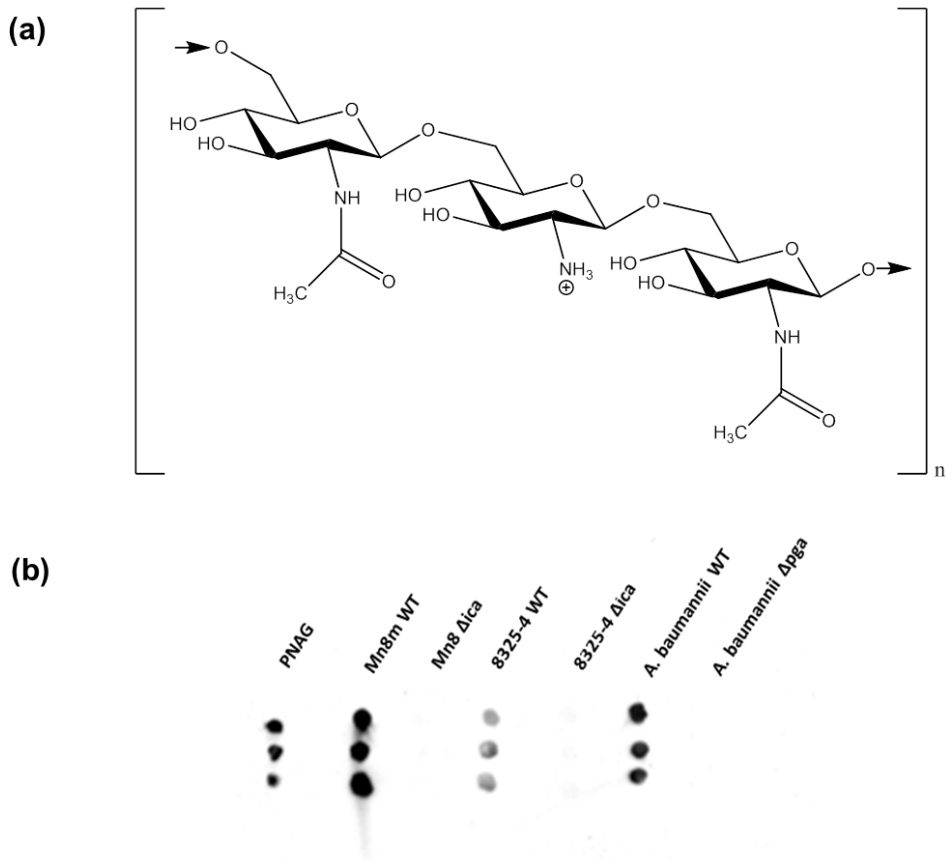

Figure 1. Structure of PNAG and verification of biofilm production under experimental conditions. (**a**) Structure of partially deacetylated poly-*N*-glucosamine (PNAG). Modifications of PNAG such as deacetylation and *O*-succinylation vary depending on bacterial genus and strain [32]. (**b**) Dot blot of heat killed *S. aureus* Mn8m, *S. aureus* 8325-4 and *A. baumannii* S1 WT and mutant strains cultured under PNAG-promoting conditions detected by anti-PNAG mAb. The same cell numbers were loaded for comparison between strains (approximately 2 x 10^6 cells).

Lectin recognition of PNAG and carbohydrate-mediated binding inhibition. WGA, which has binding specificity for both *N*-acetylglucosamine (GlcNAc) and sialic acid residues (Table S2), has been used as a 'gold standard' to detect and indicate the presence of PNAG within a biofilm matrix and on bacterial cell surfaces [33-35]. However, it has also been recognised that WGA does not exclusively recognise PNAG but also binds to other GlcNAc-containing bacterial cell surface molecules such as peptidoglycan [36-38]. As removal of PNAG in the Δ*ica*/ Δ*pga* mutant strains uncovers or exposes other abundant and prominent GlcNAc-containing structures such as peptidoglycan, which in turn then become the main contributors to lectin binding interactions, simply comparing the different binding

interactions of *Δica* or Δ*pga* mutants to WT alone will not serve to determine which lectins have preferential (but not necessarily exclusive) binding to PNAG. Therefore, to initially clarify lectin binding to PNAG alone, PNAG was purified from *S. aureus* Mn8m culture by ethanol precipitation, enzymatic digestion and size exclusion chromatography. Modifications of PNAG such as deacetylation and *O*-succinylation vary depending on bacterial genus and strain [32]. ^{1}H NMR spectroscopy confirmed the purity and identity of the PNAG preparation which was approximately 5% deacetylated (Figure S2) and not O-succinylated, consistent with the previous report [39]. Lipoteichoic acid (LTA) and peptidoglycan are major cell wall components of Gram-positive bacteria and their structure varies between species [40]. Antibody dot blots demonstrated the presence of a trace amount of LTA (0.35% (w/w)) in the PNAG preparation and confirmed that peptidoglycan was not present (Figure S3). The PNAG preparation was fluorescently labelled utilising its free amine groups (Figure 1(a)) and incubated on the lectin microarray. PNAG bound to only two lectins, sWGA, which binds exclusively to GlcNAc only (Table S2), and WGA (Figure 2(a)), and displayed a slightly higher binding intensity to WGA compared to sWGA. In agreement with these data, WGA and sWGA were previously demonstrated to bind to *S. epidermidis* 'slime', of which the major component is PNAG, using lectin histochemistry and transmission electron microscopy for detection [34]. The trace of contaminating LTA could potentially have contributed to lectin binding. However since *S. aureus* Mn8m LTA has a diglucosyl (Glc-β-(1,6)-Glc) unit and does not contain any GlcNAc [41,42], it is therefore unlikely that LTA contributed to PNAG binding to the GlcNAc-binding lectins observed here.

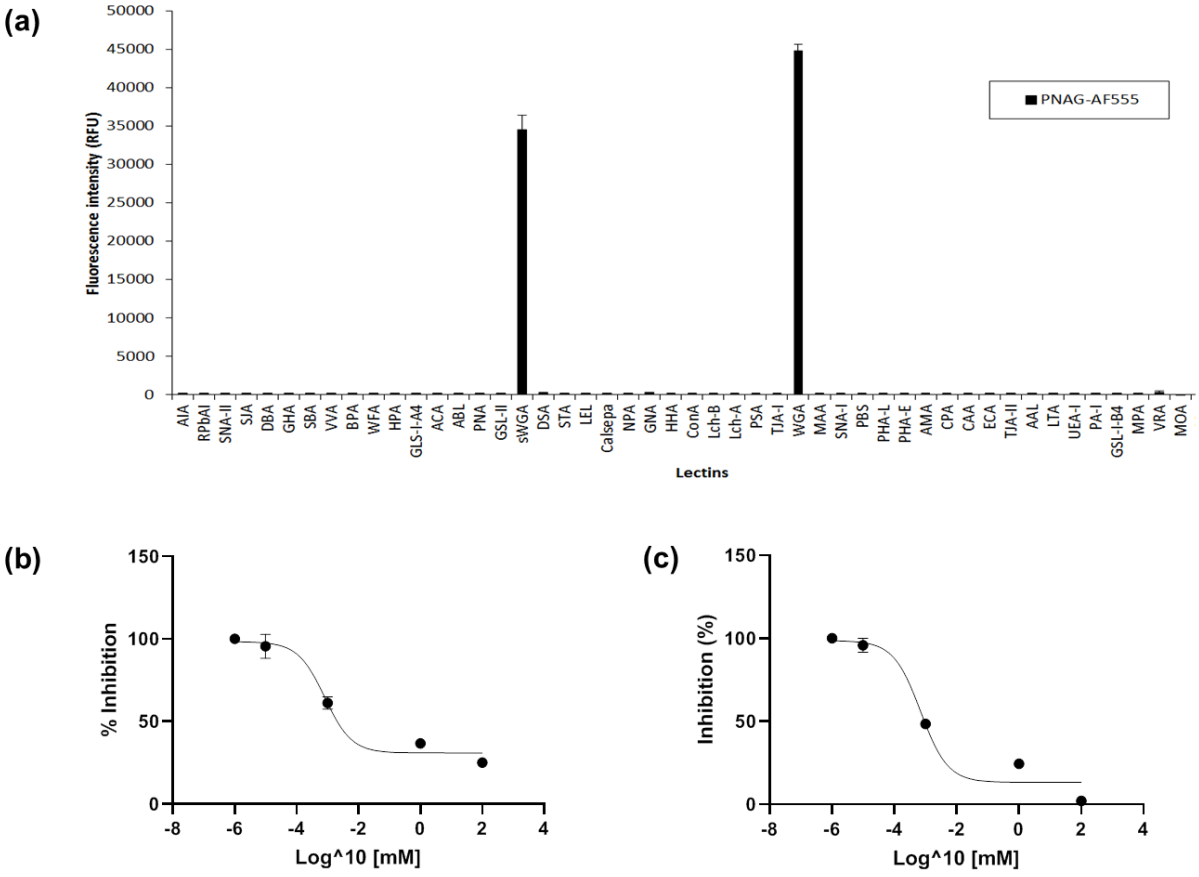

Figure 2. (**a**) Lectin microarray profile of fluorescently labelled PNAG purified from *S. aureus* Mn8m culture. Bars represent the binding intensity of the mean of three experiments with error bars of +/- 1 standard deviation (SD) of the mean. (**b**) Nonlinear fit transformation of GlcNAc inhibition PNAG binding to sWGA intensity data. Data points are the mean of three experiments with error bars of +/- 1 SD of the mean. (**c**) Nonlinear fit transformation of GlcNAc inhibition of PNAG binding to WGA intensity data. Data points are the mean of three experiments with error bars of +/- 1 SD of the mean.

Although plant lectins are often used as tools to distinguish microbes, bacterial glycosylation is quite different to mammalian glycosylation for which plant lectin specificities have been mainly characterised, and carbohydrate-mediated binding for bacterial molecules should be confirmed [20]. Free GlcNAc inhibited PNAG binding to sWGA and WGA (Figure S4), while free mannose (Man) did not as expected (not shown), confirming the specific carbohydrate-mediated binding of PNAG to the lectins. The half maximal inhibitory concentration (IC_{50}) is a measure of how effective a sugar is for inhibiting lectin binding, and in this context, a lower IC_{50} value indicates that less GlcNAc was needed to

compete for lectin binding to PNAG. The IC_{50} value generated by GlcNAc inhibition of PNAG binding to sWGA was 0.8161 μM (R^2 = 0.9732) and to WGA was 0.6995 μM (R^2 = 0.9641) (Figure 2(b) and (c)).

PNAG presentation and accessibility *in situ* on bacterial cell surface. To clarify the contribution and accessibility of cell surface retained PNAG to lectin binding of the whole bacteria, the surface glycosylation of the mutant strains were compared to the WTs cultured under the biofilm-promoting condition which produced most biofilm (Figure S1, supplemented with glucose for *S. aureus* strains BH1CC and Mn8m and *A. baumannii*, or NaCl for *S. aureus* strain 8325-4). All bacterial strains were initially titrated for optimal dye concentration for staining and cell number for incubation on lectin microarrays (Supplementary materials and Figures S5-S8). As *S. aureus* BH1CC had the lowest fluorescence following staining compared to the other two *S. aureus* strains and *A. baumannii*, an optimal cell dilution of 50 μL was selected from the *S. aureus* BH1CC lectin microarray titration (Figure S8) for consistency across strains.

In MRSA clinical isolates, glucose promotes biofilm formation *via* an *ica*-independent mechanism that involves extracellular surface proteins, such as FnBPAB, and eDNA [8,26,43]. MRSA strain BH1CC WT and Δ*ica* mutant cultured in BHI glucose exhibited overall very low binding intensities (<1,500 RFU) on the lectin microarray by comparison to the MSSA strains and *A. baumannii* (Figure 3). This may have been due to the relatively thicker cell wall of MRSA strains compared to the MSSA strains [44,45] or because that this strain had a more efficient efflux pump, and thus did not retain as much dye as the other strains. It may also indicate that the MRSA strain BH1CC cell surface glycosylation is not very accessible or prominent in this format, in addition to the overall lower dye incorporation. *S. aureus* BH1CC WT bound with greatest intensity to *Helix pomatia* agglutinin (HPA), which has specificity for α-linked GalNAc residues, GlcNAc-specific lectins *Griffonia simplicifolia* lectin-II (GSL-II), *Datura stramonium* agglutinin (DSA), which has specificity for GlcNAc residues, and *Aleuria aurantia* lectin (AAL), which has specificity for α-(1,6)- and α-(1,3)-linked Fuc residues and *Maclura pomifera* agglutinin (MPA), which has specificity for terminal α-linked Gal residues, but only moderate binding intensity was observed with sWGA and WGA (Table S2 and Figure 3(a)). While bacterial carbohydrate binding may not correspond exactly with the specificities for lectin established based on mammalian-type glycosylation, it is clear that these data indicated that PNAG and

GlcNAc-containing molecules were not main contributor(s) to *S. aureus* BH1CC WT cell surface or biofilm glycosylation, which is in agreement with the established absence of PNAG on the MRSA cell surface [8]. Additionally, the Δ*ica* mutant demonstrated slightly decreased binding to HPA, sWGA and GSL-II (Figure 3(a)). Although these changes in binding instensity were statistically significant, they were very slight in absolute intensity (<500 RFU) and thus likely indicated only very minor changes to surface glycosylation in the MRSA BH1CC Δ*ica* mutant compared to WT.

When cultured supplemented in 4% NaCl, *S. aureus* 8325-4 WT bound with greatest intensity to the GlcNAc-specific lectins GSL-II, WGA and sWGA, with highest binding to GSL-II (Table S2 and Figure 3(b)). There was an overall trend of decreased binding of *S. aureus* 8325-4 Δ*ica* to all lectins compared to the WT, but only the decreased binding to GSL-II was significant (Figure 3(b)). It is unlikely that GSL-II binding of the *S. aureus* 8325-4 WT was due to PNAG alone, as PNAG alone did not bind to GSL-II (Figure 2(a)). Instead, the decreased binding of the Δ*ica* mutant to GSL-II was likely due to GSL-II binding to another GlcNAc-containing surface molecule such as peptidoglycan or teichoic acid, binding which was augmented by the presence of PNAG in the WT. This kind of altered or modulated binding due to 'neighbouring effects' has been previously reported for anti-stage specific embryonic antigen 3 (SSEA3, Gb5) antibody interactions [46]. From these data, it is clear that PNAG and other cell surface molecules were accessible and available for binding interactions, and PNAG did not completely obscure the cell surface from molecular interactions even under biofilm-producing conditions. Alternatively, some additional cell surface molecules may be secreted into the biofilm matrix and presented for binding along with the PNAG. The suggestion of incomplete surface coverage of *S. aureus* 8325-4 by PNAG is further supported by previous reports featuring electron microscopy images of *Staphylococcus* species in a biofilm matrix which showed incomplete bacterial surface coverage by biofilm components [10,34,47].

On the other hand, *S. aureus* Mn8m produced approximately 3 times more PNAG than the 8325-4 strain (205% more PNAG compared to *S. aureus* 8325-4 by densitometry, Figure 1(b)), so PNAG may more fully enclose the strain Mn8m bacterial cell surface under biofilm-promoting conditions. *S. aureus* Mn8m WT bound with greatest intensity to the lectins GSL-II, sWGA and WGA, with WGA binding of greatest relative intensity (Figure 3(c)). Binding to WGA and GSL-II was decreased for the *S. aureus* Mn8 Δ*ica* mutant

compared to Mn8m, and sWGA binding was entirely absent for the mutant (Figure 3(c)). Thus sWGA binding of the MSSA Mn8m WT was entirely due to PNAG alone and no exposed surface molecules of the WT interacted with sWGA in addition to PNAG, supporting the proposal of more complete obscuring of the *S. aureus* Mn8m WT cell surface compared to *S. aureus* 8325-4 WT. Therefore, depending on surface coverage, PNAG may not be the most prominent molecule contributing binding interactions and/or it may serve to modulate binding of recognition molecules to cell surface components.

A. baumannii S1 WT grown in biofilm-inducing glucose demonstrated binding to *Dolichos biflorus* agglutinin (DBA), which has specificity for GalNAc residues, *Amaranthus caudatus* agglutinin (ACA), for sialylation and Gal-β-(1,3)-GalNAc, WGA, *Arum maculatum* agglutinin (AMA), for Gal-β-(1,4)-GlcNAc (*N*-acetyllactosamine (LacNAc)), *Cicer arietinum* agglutinin (CPA), for complex oligosaccharides, and *Vigna radiata* agglutinin (VRA), which has specificity for terminal α-linked Gal residues, of which the most intense binding was to DBA, CPA and VRA (Table S2 and Figure 3(d)). If lectin specificities for bacterial glycosylation are as previously characterised, this could indicate that *A. baumannii* has a cell surface rich in Gal and GalNAc-containing structures. Given the relatively lower binding to WGA and sWGA, this shows that PNAG is not the most prominent cell surface presented molecule for *A. baumannii* and it is relatively less accessible for interactions compared to MSSA strains under biofilm-promoting conditions.

Interestingly, *A. baumannii* Δ*pga* demonstrated reduced binding to DBA, ACA, CPA and VRA in comparison to the WT, but not to WGA, sWGA or any other GlcNAc-specific lectins (Figure 3(d)). The lack of reduction in binding to GlcNAc-specific lectins for the mutant strain indicates that, even aside from relatively minor structural differences in terms of degree of deacetylation, PNAG was presented quite differently on the surface of *A. baumannii* compared to the MSSA strains. Although PNAG on both MSSA and *A. baumannii* surfaces was detectable by a recognition molecule specific for PNAG, the anti-PNAG mAb (Figure 1(b), recognition molecules that were not specific for PNAG such as innate immune receptors may not bind to PNAG presented in a different manner or that is accessible in a different orientation, as demonstrated by the plant lectins here. Since DBA, ACA, CPA and VRA lectins mainly have specificity for Gal and GalNAc residues, these data suggest that the role of PNAG on the surface of *A. baumannii* may be to influence or modulate the presentation of other cell surface components, such as lipopolysaccharides

(LPS) or capsular polysaccharide (CPS). For example, CPS isolated from *A. baumannii* NIPH146 had a pentasaccharide repeating unit composed of Glc, Gal and GalNAc residues which contained a α-D-Gal*p*-(1,6)-β-D-Glc*p*-(1,3)-D-Gal*p*NAc trisaccharide fragment common among many *A. baumannii* strains [48], and the O-antigen isolated from *A. baumannii* strain 9 and ATCC 17961 LPSs consisted of Glc, GalNAc, Gal, GlcNAc and GlcNAc3NAcA residues [49]. Therefore, PNAG may have a role in modulating the interactions of other more prominent molecules of the *A. baumannii* surface with recognition molecule(s), rather than PNAG itself directly interacting with recognition molecules.

Taking all of the above in to account, it is not advisable to exclusively use WGA as the sole method for specifically identifying the presence of PNAG in biofilm or on cell surfaces. Instead, we suggest that sWGA may be a better indicator for the presence of PNAG in *S. aureus* cultures or biofilms, but using a recognition molecule that is specific for the PNAG structure itself such as a mAb for PNAG may be the best identification molecule across bacterial species. However, as demonstrated here, the use of the antibody alone cannot show conformational or presentation differences and should be combined with a multi-interaction detection platform such as the lectin microarray for a more complete understanding.

Overall these data demonstrate differences in surface presentation and accessibility of PNAG *in situ* on the bacterial cell surface, with complete surface coverage by PNAG indicated for MSSA Mn8m, incomplete PNAG surface coverage for MSSA 8325-4 with accessibility of other cell surface molecules for interactions, no PNAG on the MRSA cell surface as expected, and, although PNAG was present on *A. baumannii* cell surface, other surface molecules were the most accessible on *A. baumannii* and PNAG influenced their interactions.

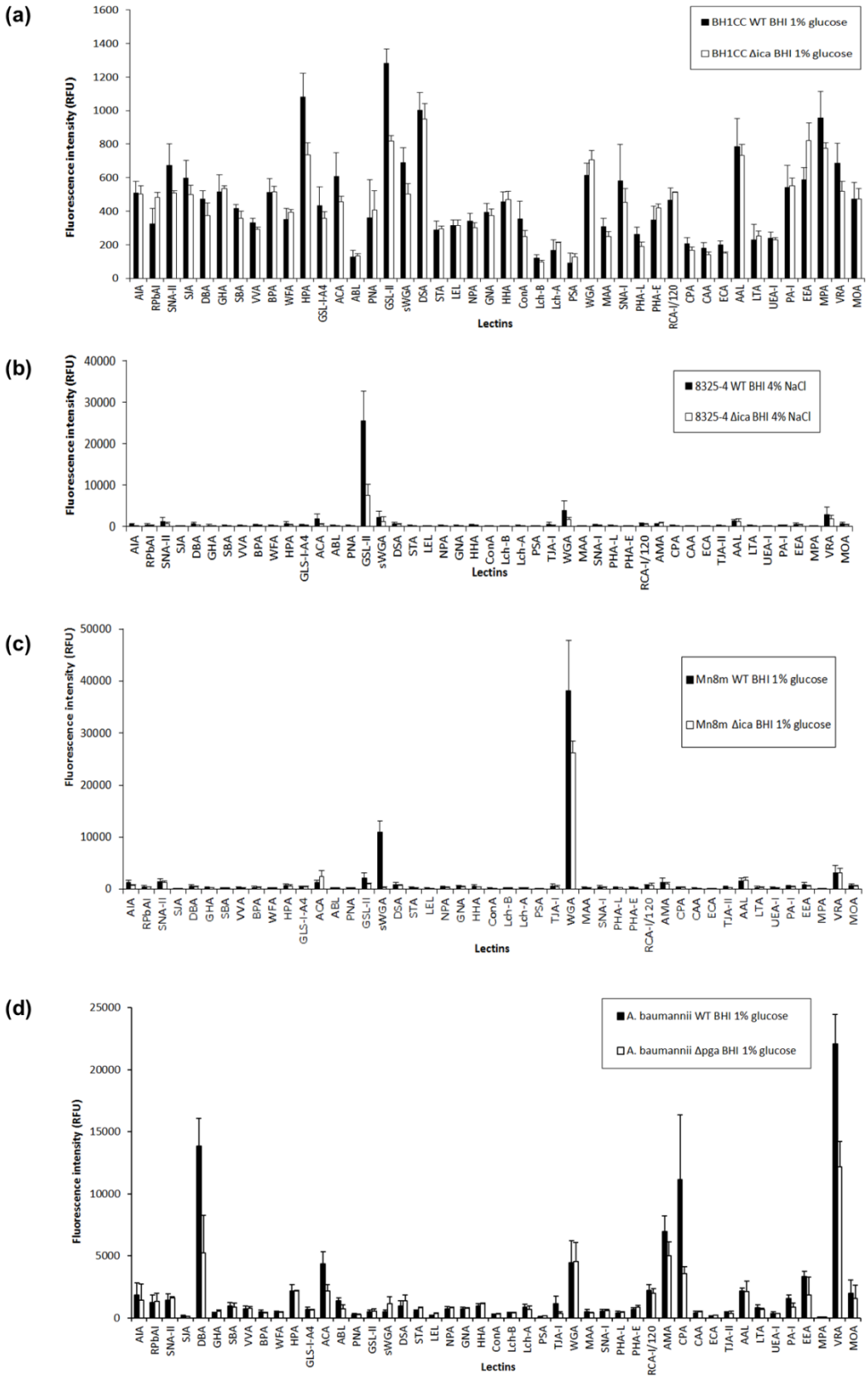
(a)
Fluorescence intensity (RFU)
BH1CC WT BHI 1% glucose
BH1CC Δica BHI 1% glucose
Lectins
(b)
Fluorescence intensity (RFU)
8325-4 WT BHI 4% NaCl
8325-4 Δica BHI 4% NaCl
Lectins
(c)
Fluorescence intensity (RFU)
Mn8m WT BHI 1% glucose
Mn8m Δica BHI 1% glucose
Lectins
(d)
Fluorescence intensity (RFU)
A. baumannii WT BHI 1% glucose
A. baumannii Δpga BHI 1% glucose
Lectins

Figure 3. Surface glycosylation profiles of WT bacterial strains grown in BHI media supplemented with glucose or NaCl. Bar charts represent binding intensities of bacteria to lectins on the lectin microarray. (**a**) *S. aureus* BH1CC WT and *Δica* mutant bacterial strains grown in BHI media with 1% glucose, (**b**) *S. aureus* 8325-4 WT and *Δica* mutant bacterial strains grown in BHI media with 4% NaCl, (**c**) *S. aureus* Mn8m and Mn8 *Δica* mutant bacterial strains grown in BHI media with 1% glucose, and (**d**) *A. baumannii* WT and Δ*pga* grown in BHI media with 1% glucose. Bars represent the mean of three experiments with error bars of +/- 1 SD of the mean.

Carbohydrate specificity of *A. baumannii* and *S. aureus* strains. We next investigated the specificity of carbohydrate binding of *S. aureus* [50] and *A. baumannii* using carbohydrate microarrays (Tables S3 and S4). All WT and mutant strains were grown in biofilm-promoting conditions as for lectin microarray profiling. Additionally, MRSA BH1CC was also cultured with NaCl supplementation as salt inclusion promotes *icaA* transcription but does not promote biofilm formation in MRSA clinical isolates [8], and this condition would be useful to compare to the *ica*-independent mechanism promoted by inclusion of glucose that involves extracellular surface proteins, such as the fibronectin-binding protein (FnBP) FnBPAB, and eDNA [8,26,43]. For comparison, the MSSA strain 8325-4 was also grown in the presence of glucose which also increases PNAG-mediated biofilm formation in this strain.

Overall, the most intensely binding ligands for MSSA strain 8325-4 WT cultured in BHI glucose were 3'-sialyllactose (3SLac, on neoglycoconjugate 3SLacHSA), 6'-sialyllactose (6SLac, on neoglyconjugate 6SLacHSA), H type II (H2, on neoglycoconjugate H2BSA), lacto-*N*-tetraose (LNT, on neoglycoconjugate LNTHSA), rhamnose (Rha, on neoglycoonjugate RhaBSA), α-linked mannose (Man, on neoglycoconjugate XManaBSA) and β-linked Glc (on neoglycoconjugate GlcbITCBSA) (Figure S9, Tables S3 and S4). When cultured in BHI NaCl, the binding pattern of *S. aureus* 8325-4 WT remained similar with the most intense binding including the glycoprotein α-crystallin (a-C) and difucosyl-para-lacto-*N*-hexaose (DFPLNH, on the neoglycoconjugate DFPLNH) (Figure S10, Tables S3 and S4). The other MSSA strain Mn8m WT cultured in BHI glucose had a similar binding pattern to strain 8325-4 cultured under both conditions and bound most intensely to similar ligands

including a-C, 3SLac, 6SLac, H2, DFPLNH, LNT, Rha, α-linked Man and β-linked Glc, and additionally Lewis b (Leb, on neoglycoconjugate LebBSA) (Figure S11, Tables S3 and S4).

For the MRSA strain BH1CC cultured in BHI glucose the overall binding intensities to carbohydrates were greater than overall lectin binding intensity and were comparable in intensity to the MSSA strains. The most intense binding for *S. aureus* BH1CC cultured in BHI glucose was for ligands 3SLac, 6SLac, H2, DFPLNH, LNT, Rha, α-linked Man and β-linked Glc (Figure 4(a), Tables S3 and S4). When cultured in BHI NaCl, *S. aureus* strain BH1CC exhibited markedly lower overall intensity (<2,000 RFU), which may correspond with the much greater quantity of biofilm produced when *S. aureus* BH1CC is cultured in glucose compared to salt (Figure S1C). The most intensely binding ligands for this strain cultured with NaCl were the 4-aminophenyl linker (4AP, on the protein conjugate 4APHSA), a-C, 3SLac, 6SLac, H2, LNT, Rha, α-linked Man and β-linked Glc (Figure 4(b)). Although not among the most intensely binding ligands, under both culture conditions *S. aureus* BH1CC bound with moderate relative intensity to human matrix protein fibrinogen (fibrin, Tables S3 and S4) but very low relative intensity to fibronectin. Binding to fibrinogen was much greater in absolute intensity when cultured in glucose (approximately 3,000 RFU, Figure 4(a)) compared to culturing in NaCl (approximately 200 RFU, Figure 4(b)). This may be due to the greater quantity of FnBPAB-mediated biofilm production under the glucose supplemented growth condition as expected (Table 1 and Figure S1(c)). Although FnBPAB is known to be produced by *S. aureus* BH1CC (Table 1), it may not be among the most intensely binding ligands for this strain as the major biofilm component is eDNA rather than FnBPs [27].

Similarly to the *S. aureus* strains, *A. baumannii* WT cultured in BHI glucose bound most intensely to 3SLac, 6SLac, H2, LNTHSA, Rha, α-linked Man and β-linked Glc (Figure 5).

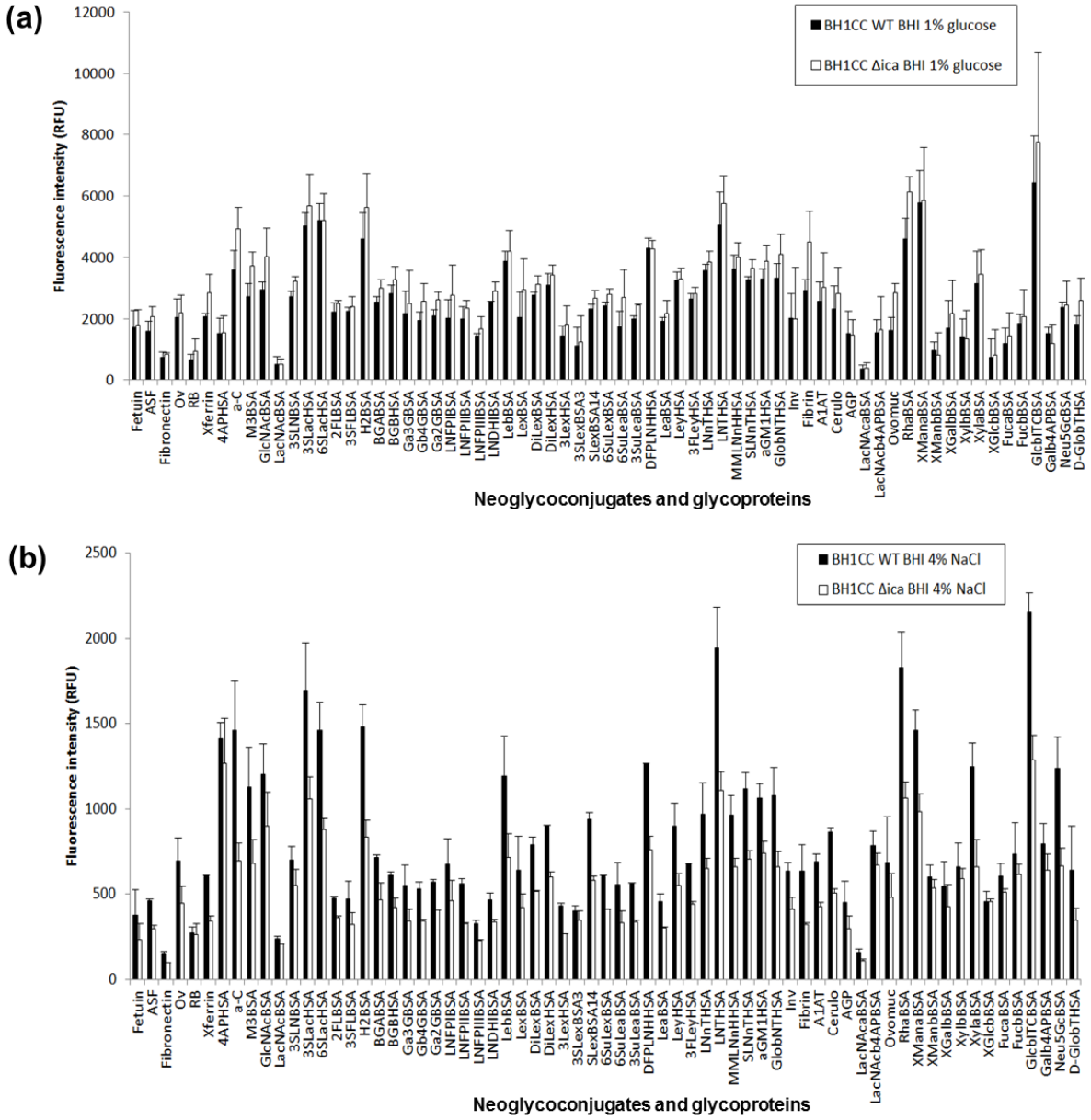

Figure 4. Carbohydrate microarray binding intensity profiles of *S. aureus* BH1CC WT and Δ*ica* grown in BHI supplemented with (**a**) 1% glucose and (**b**) 4% NaCl. Bars represent the mean of three experiments with error bars of +/- 1 SD of the mean.

For all strains, the binding to Rha is unlikely to be biologically relevant to human infection as Rha is a common component in plants and some bacteria (e.g. Mycobacterium) but does not occur in mammals, and indeed the linker may contribute to binding here. All strains also bound to β-linked Glc and α-linked Man, but only when the phenylisothiocyanate

(ITC) linker was present. None of the strains bound with similar high intensity to β-linked Glc when it was presented with the 4AP linker (XGlcbBSA, Tables S3 and S4) nor to the α-linked Man presented as part of the Man-α-(1,3)-[Man-α-(1,6)-]Man trisaccharide structure (M3BSA) or in the high mannose structures on the glycoprotein ribonuclease B (RB, Tables S3 and S4). The influence of the phenylisothiocyanate (ITC) linker on carbohydrate binding has been previously reported where Con A lectin, which normally has binding specificity for α-linked Man and Glc (Table S2), bound to Glc which was β-linked with a phenylazo linker [51]. Thus, we hypothesize that the ITC linker is particularly accessible in these ITC-linked neoglycoconjugates and the interactions with bacteria were mediated, at least in part, by the ITC linker and not dependent on carbohydrate binding.

Inhibition studies using free mono- or oligo-saccharides were not used here to verify carbohydrate-mediated bacterial binding as many bacteria can ferment free carbohydrates and this can change the expression of surface molecules (e.g. glucose supplementation increases *S. aureus* biofilm expression as demonstrated in this work). Alternatively, structural specificity can be deduced and confirmed by including closely related structural variations or different presentations in the presented ligand panel, as demonstrated in the case above of the strains binding to α-linked Man on the ITC linker but not α-linked Man presented on the trisaccharide M3BSA or on RB, indicating that bacterial binding was not dependent on the carbohydrate in the case of neoglycoconjugate XManaBSA.

All strains appeared to favour binding to sialylated type II lactose (Lac, Gal-β-(1,4)-Glc) and 3SLac, but not to 3'sialyl-*N*-acetyllactosamine (3'SLacNAc, Neu5Ac-α-(2,3)-Gal-β-(1,4)-GlcNAc, on the neoglycoconjugate 3SLNBSA, Table S3). Therefore the *N*-acetylamino group on 3'SLacNAc may be inhibitory to binding. None of the strains favoured intense binding to unmodified LacNAc (Gal-β-(1,4)-GlcNAc, on the neoglycoconjugates LacNAcBSA, LacNAcaBSA and LacNAcb4APBSA, Tables S3 and S4) either. However, when LacNAc was substituted with terminal α-(1,2)-linked fucose (Fuc) in the H2 antigen (Fuc-α-(1,2)-Gal-β-(1,4)-GlcNAc), relatively intense binding occurred. This favoured binding to terminal α-(1,2)-linked Fuc was supported by moderate to intense binding of Leb (Fuc-α-(1,2)-Gal-β-(1,3)-[Fuc-α-(1,4)-]GlcNAc-β-(1,3)-Gal-β-(1,4)-Glc) by all strains. Interestingly, the Leb structure on a different neoglycoconjugate, LNDHIBSA, was not bound by the strains as intensely as LebBSA. This may be due to the higher substitution of Leb on the BSA backbone on LebBSA compared to LNDHIBSA (substitution of 10

compared to 7.5 (range 4-12), respectively) as even small differences ligand density can dramatically affect avidity of the interactions [52]. The different linkers of LebBSA and LNDHIBSA may also have a role in ligand presentation differences, but the effect may not have as much impact on the conformation or accessibility of longer oligosaccharides compared to monosaccharides.

The species and strains differed more in their moderate to low intensity binding. For example, all *S. aureus* WT strains in all culture conditions had low relative binding to Lewis x (Lex, on the neoglyconjugate LexBSA), blood group B (BGB, on neoglyconjugate BGBBSA) and blood group A (BGA, on neoglyconjugate BGABSA) (Figures 4 and S9-S11), all of which do not have terminal α-(1,2)-linked Fuc, while *A. baumannii* WT also had low Lex binding but moderate binding to BGA and BGB (Figure 5B). Thus, these bacterial strains may have preferential binding to secretor hosts that have a functional *FUT2* gene, which makes the enzyme α-1,2-fucosyltransferase, rather than non-secretors who have a non-functional *FUT2* gene. Fucosylation plays an important role for host-microbe interactions and secretor status is a genotypic factor that contributes to microbial diversity, particularly bifidobacteria diversity, in the intestinal microbiota [53]. Tissue specific expression of histo-blood group antigens indeed appears to influence *S. aureus* colonisation. Non-secretors of blood group O are more likely to carry S. aureus in their throat compared to blood group A non-secretors, while secretors of blood group O appear to be protected [54]. The latter may be due to the production of mucus containing α-(1,2)-linked Fuc-expressing mucins in blood group O secretors constantly removing resident *S. aureus* from the throat with mucus turnover. In addition, although some strains of *S. aureus* have been shown to bind to Lewis a (Lea) via a specific adhesin [55], binding to Lea (on the neoglycoconjugate LeaBSA) was relatively low intensity for all *S. aureus* strains and growth conditions assessed in this work, so Lea binding may be strain-specific. To the best of our knowledge, *A. baumannii* colonisation or infections have not been associated with histo-blood groups to date.

The WT MSSA strains cultured in glucose did not bind to either fibronectin or fibrinogen (relatively very low intensity binding, Figures S9 and S11) while *S. aureus* 8325-4 cultured with NaCl exhibited relatively low to moderate binding intensity (Figure S10) despite the known presence of FnBPs in *S. aureus*, which bind to both fibronectin and fibrinogen [56]. The relevant FnBP adhesins may not have been abundantly expressed without the presence of fibrinogen or fibronectin and under these culture conditions.

Alternatively, the *S. aureus* binding demonstrated in this work may reflect that *S. aureus* binding to the other presented ligands is actually relatively more intense or important than fibrinogen or fibronectin binding. Certainly this is likely in the case of *S. aureus* BH1CC, where the majority biofilm component is eDNA and not FnBPAB [27].

Bacterial lectin function in *A. baumannii* biofilm assembly. Removal of PNAG may result in an overall increased or decreased carbohydrate binding of the mutants compared to WTs, but not result in a difference in relative binding pattern. This may be due to reduced overall 'stickiness' of the bacterium with the loss of the PNAG or differences in the degree of dye uptake, which can affect the overall fluorescence of the bacteria and result in a 'shelving effect' despite loading the same cell number. Such a 'shelving effect' would be an artefactual difference in overall binding intensity and not representative of real binding differences between strains or conditions. To examine whether any carbohydrate binding was altered between the WT and Δ*ica* and Δ*pga* mutants and also mitigate against any bias introduced by potential artefactual differences, we first compared the scale normalised carbohydrate binding profiles of all strains by hierarchical clustering (Figure 5(a)) to identify lectin functions that could play a role in biofilm assembly. Overall binding patterns that are different can then be subjected to testing individual binding interactions for statistical significance between the WT and mutant. This approach for identifying differences with potential biological consequence is particularly relevant to complex systems such as bacteria, which are more likely to have multiple surface lectins with different specificities and affinities that are expressed in different ratios under different conditions, rather than the much simpler 'on-off' or 'binding-no binding' approach, which is a more suitable approach for simple or single component systems.

Two major groups were created by unsupervised hierarchical clustering, with one group containing both WT and Δ*ica* mutant MSSA strains, under all culture conditions, and the other group containing the MRSA strain WT and Δ*ica* mutant, under all culture conditions. The Δ*ica* mutants of *S. aureus* strains 8325-4 and Mn8m and the Mn8m WT when cultured in BHI glucose were essentially the same (90% similarity, Figure 5(a)), and also had high similarity to the S. aureus 8325-4 WT cultured in glucose, despite apparent differences of absolute intensity (rather than relative intensity) for strain 8325-4 (Figures S9). *S. aureus* 8325-4 WT and Δ*ica* when cultured in BHI NaCl were a little different in overall binding pattern compared to when cultured in BHI glucose (70% similarity, Figure 5(a)).

Binding of the *S. aureus* 8325-4 Δ*ica* mutant sultured in BHI NaCl was significantly ($p \leq 0.05$) increased compared to the WT to several structures: the H2 antigen (on the neoglycoconjugates H2BSA and 2FLBSA), Gal-β-(1,4)-Gal (on the neoglycoconjugate Gb4GBSA), Lewis y (Ley, on the neoglycoconjugate LeyHSA), monofucosyl monosialyllacto-*N*-neohexaose (on the neoglycoconjugate MMLNnHHSA) and α-linked Man (on the neoglycoconjugate XManaBSA, which is Man-α-ITC-BSA) (Figure S10). However, several of these significantly different bindings were not substantially different in magnitude. The only substantially increased binding (≥50%) of the Δ*ica* mutant compared to *S. aureus* 8325-4 WT was to fibronectin (139%), fibrinogen (102%), α-linked Man (on the neoglycoconjugate XManaBSA), β-linked Gal (87%, on the neoglycoconjugate XGalbBSA (Gal-β-ITC-BSA)) and β-linked Glc (61%, on the neoglycoconjugate GlcbITCBSA) (Figure S10). As discussed above in the previous section, the ITC linker may have a role in the substantially increased binding to the α-linked Man, β-linked Gal and β-linked Glc as these large increases in binding were not observed for the same carbohydrates on different linkers or presentations. However, the altered binding to fibronectin and fibrinogen may indicate the increased importance of FnBP adhesins in biofilm assembly for *S. aureus* 8325-4 under these culture conditions.

Within the second group containing MRSA, the similarity of *S. aureus* BH1CC WT and Δ*ica* cultured in BHI glucose (86%, Figure 5(a)) showed that the binding pattern was essentially the same, with the same conclusion for *S. aureus* BH1CC WT and Δ*ica* cultured in BHI NaCl (79%, Figure 5(a)). However, the binding pattern differed for *S. aureus* BH1CC when cultured in NaCl compared to glucose supplementation. These differences were mainly in relative intensity of binding to the moderately bound ligands, including lower binding of the BHI NaCl culture to fibrinogen, 6-sulfoLewis x (6SuLex, on neoglycoconjugate SuLexBSA) and the 4AP linker. The overall similarity of carbohydrate binding pattern between the WT and mutants of the same *S. aureus* strains indicates that surface bound or secreted adhesins with lectin function are not likely to have an important role in biofilm assembly or surface presentation for this species. In addition, these data demonstrate that different culture conditions impacts on binding pattern, likely influencing the relative ratios of surface lectins produced rather than a simple ‘on-off’ expression.

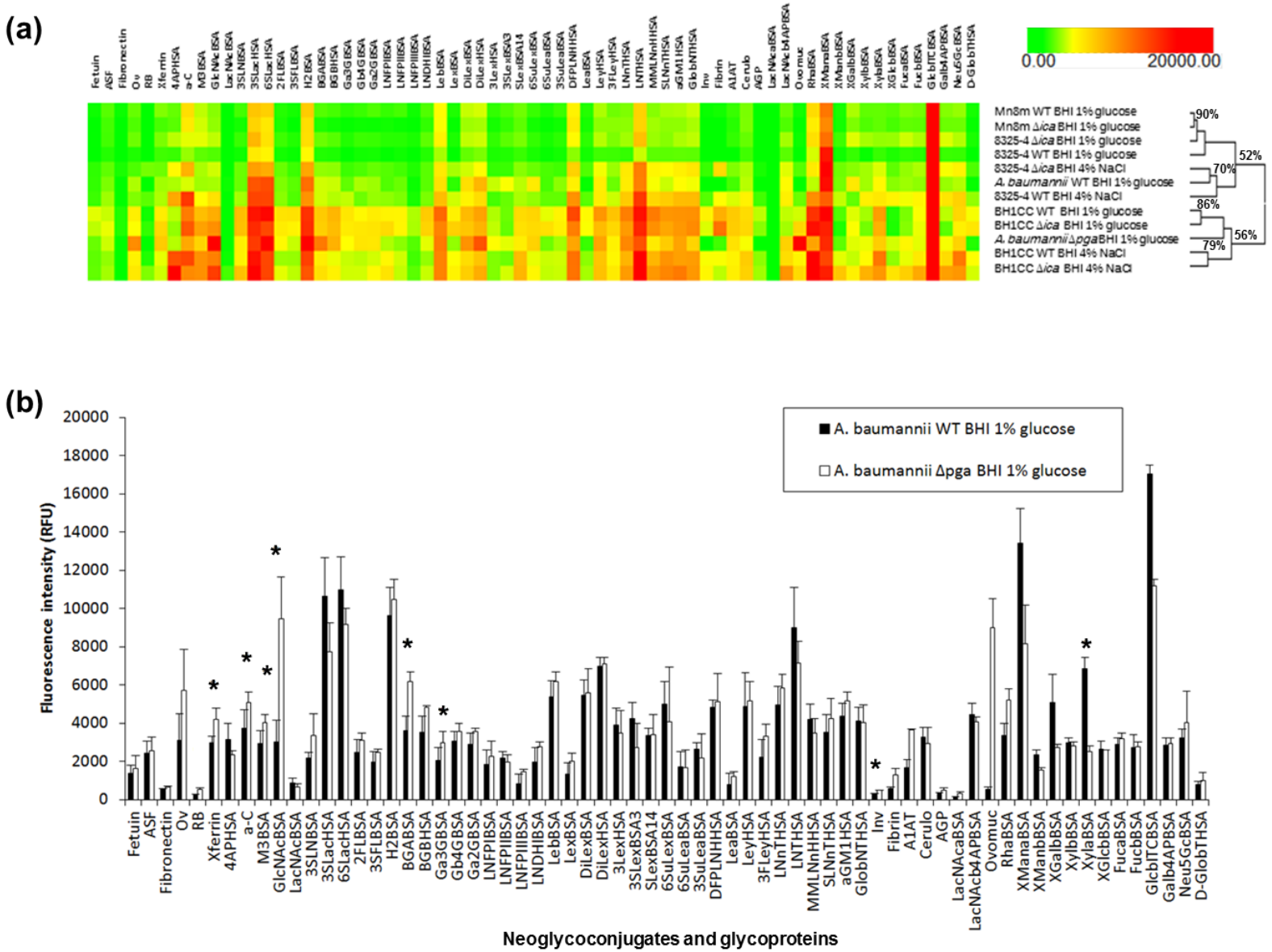
(a)
0.00
20000.00
Mn8m WT BHI 1% glucose
Mn8m Δica BHI 1% glucose
8325-4 Δica BHI 1% glucose
8325-4 WT BHI 1% glucose
8325-4 Δica BHI 4% NaCl
A. baumannii WT BHI 1% glucose
8325-4 WT BHI 4% NaCl
BH1CC WT BHI 1% glucose
BH1CC Δica BHI 1% glucose
A. baumannii ΔpgaBHI 1% glucose
BH1CC WT BHI 4% NaCl
BH1CC Δica BHI 4% NaCl
90%
52%
70%
86%
56%
79%
(b)
A. baumannii WT BHI 1% glucose
A. baumannii Δpga BHI 1% glucose
Fluorescence intensity (RFU)
Neoglycoconjugates and glycoproteins

Figure 5. Carbohydrate binding instensities of bacterial strains. (**a**) Unsupervised hierarchical clustering of carbohydrate microarray binding intensities for *S. aureus* Mn8m, 8325-4, BH1CC and *A. baumannii* all grown in BHI supplemented with 1% glucose, and supplemented with 4% NaCl for *S. aureus* 8325-4 and BH1CC. Binding intensity data was scale normalised to a range of 0-20,000 RFU and clustered using Hierarchical Clustering Explorer v3.0 with complete linkage and Euclidean distance. (**b**) Bar chart representing carbohydrate binding intensities of *A. baumannii* WT and Δ*pga* grown in BHI glucose. Bars represent three experiments with error bars of +/- 1 SD of the mean of the three experiments. * represents significant difference ($p \leq 0.05$, calculated by student's t test, two tailed) in binding between WT and Δ*pga*.

A. baumannii WT and Δ*pga* mutant clustered separately in to the two different major groups, with the WT clustering with the PNAG-producing MSSA strains and conditions and *A. baumannii* Δ*pga* clustering with the non-PNAG producing MRSA group (Figure 5(a)). *A. baumannii* Δ*pga* demonstrated significantly ($p \leq 0.05$) increased binding in comparison to WT for the neoglycoproteins GlcNAcBSA, M3BSA, 3SLacHSA, Ga3GBSA, BGABSA, XylaBSA and GlcbITCBSA, and the glycoproteins ovalbumin (Ov), α-crystallin (a-C), transferrin (Xferrin) and invertase (Inv) (Figure 5(b), Tables S3 and S4). However, some of these binding differences were negligible in magnitude despite their statistical significance. Substantially increased binding (≥50%) for *A. baumannii* Δ*pga* was observed for the probes Ov (83%), GlcNAcBSA (212%), LexBSA (50%), RB (115%), 3SLNBSA (55%), BGABSA (71%), LNFPIIIBSA (71%), Inv (76%), human fibrinogen (116%), human alpha-1 antitrypsin (A1AT, 120%), LacNAcaBSA (128%), ovomucoid (ovomuc, 1,522%), and RhaBSA (55%) (Figure 5(b)) in comparison to the WT, while GM1HSA (-135%) and XylaBSA (-63%) exhibited substantially decreased binding in comparison to the WT.

The most substantial increase in binding of *A. baumannii* Δ*pga* was to ovomucoid from chicken egg white which has mainly tri- and penta-antennary complex-type N-linked glycans, with the most abundant structures having mainly terminal GlcNAc residues and almost 80% of structures have bisecting GlcNAc [57]. Bacterial binding specificity for terminal β-linked GlcNAc residues was further supported by the substantially increased binding to GlcNAcBSA (which was also statistically significant) and A1AT. A1AT from healthy human plasma has complex type N-linked glycosylation with mainly biantennary structures and some tri- and tetra-antennary. The majority of structures have terminal sialylation and galactosylation but a proportion of the biantennary structures have terminal GlcNAc residues and bisecting GlcNAc. In addition, A1AT glycosylation has been shown to be altered with chronological age and to differ between males and females [58]. Thus, the *A. baumannii* Δ*pga* binding specificity for several carbohydrate structures was revealed, including terminal β-linked GlcNAc residues by the substantially increased binding to GlcNAcBSA, ovomucoid and A1AT compared to the WT.

The GlcNAc-binding lectin functionality of *A. baumannii* revealed by the removal of PNAG may have a functional role in binding PNAG tightly to the bacterial cell surface, making it less accessible for recognition molecules that are not specific for PNAG but influencing the

presentation or accessibility of other cell surface molecules such as LPS. In *S. aureus*, PNAG is deacetylated by approximately 5% [39] imparting an overall positive charge. In biofilm formation, it has been postulated that electrostatic interactions play a crucial role in biofilm formation. For biofilms that are dependent on extracellular surface proteins, such as those formed by MRSA, it has been proposed that eDNA acts as an electrostatic net that connects positively charged surface proteins in low pH environments within a biofilm matrix [59]. There are also many negatively charged molecules on the surface of bacteria, including teichoic acids, which imparts an overall negative charge on the bacterial cell surface. Thus it has been hypothesised that the positively charged amine groups on PNAG act as an electrostatic glue that interacts with these negative charges, helping to hold a biofilm matrix together [47] and thereby immobilising and presenting the PNAG on the *S. aureus* cell surface. However, *A. baumannii* PNAG is deacetylated by approximately 40% [28], and so has a correspondingly higher charge while the Gram-negative bacterial cell surface is also typically negatively charged. Interestingly, it has been reported that Gram-negative strains that adhered to a positively charged surface ceased to grow, but there was no antimicrobial effect on Gram-positive bacteria [60]. Direct contact of this higher charge with the surface of the Gram-negative bacteria may be antimicrobial, so an 'anchor' to keep the PNAG close to the surface but not touching it could be the required function fulfilled by the GlcNAc-binding surface lectin in *A. baumannii*.

There are many bacterial surface-bound proteins with adhesin and lectin function involved in biofilm formation and organisation, including FnBPs and Protein A, which contains the GlcNAc-binding module LysM [61]. However no *S. aureus* lectins have been found to directly associate with PNAG to promote biofilm formation, in agreement with our data. Mutation of *lysM* in *A. baumannii* reduces biofilm formation [62], which supports a role for this GlcNAc-binding module for *A. baumannii* biofilm formation and thus LysM may be a promising candidate for the GlcNAc-binding lectin identified in this work.

Differential surface presentation of PNAG on *A. baumannii* and *S. aureus*. The differential surface presentation of *A. baumannii* PNAG compared to *S. aureus* indicated by the carbohydrate binding data is in agreement with the different surface presentation and accessibility of PNAG between the species indicated by the lectin binding data. Based on the lectin microarray data, the surface molecules of MSSA strain 8325-4 were accessible and

contributed to binding interactions, which suggested incomplete PNAG coverage of the bacterial cell surface (Figure 6(a)), similar to the partial surface coverage by biofilm previously indicated in scanning electron microscopy images of *S. epidermidis* with intact PNAG on the cell surface [10,63].

On the other hand, the highly deacetylated *A. baumannii* PNAG may support tight adherence to the cell surface, with the GlcNAc-binding lectin(s) occupied in anchoring the PNAG to the cell surface and providing a buffer to block direct contact between the highly charged polysaccharide and the cell surface. From our lectin microarray data, it is clear that PNAG is not the main surface molecule accessible by non-specific environmental recognition molecules, but it did influence the presentation and accessibility of the other surface molecules of *A. baumannii*, likely including LPS. Thus we propose a model for PNAG presentation on the *A. baumannii* surface where PNAG is tightly adherent to the cell surface but not touching it and other surface molecules extend beyond the immobilised PNAG, with PNAG influencing their presentation (Figure 6(b)).

The differentially presented PNAG on *A. baumannii* and *S. aureus* surfaces may help the PNAG perform different biological roles or physical functions for each species. For example, compared to *S. aureus*, PNAG on the surface of *A. baumannii* appears to play a role in biofilm integrity under shear force, whereas PNAG on MSSA plays a vital role in biofilm formation under static conditions [28]. Furthermore, the tightly adherent PNAG on the *A. baumannii* surface may contribute to its extraordinarily long survival time on abiotic surfaces under desiccated conditions, contributing to its persistence in clinical environments [64].

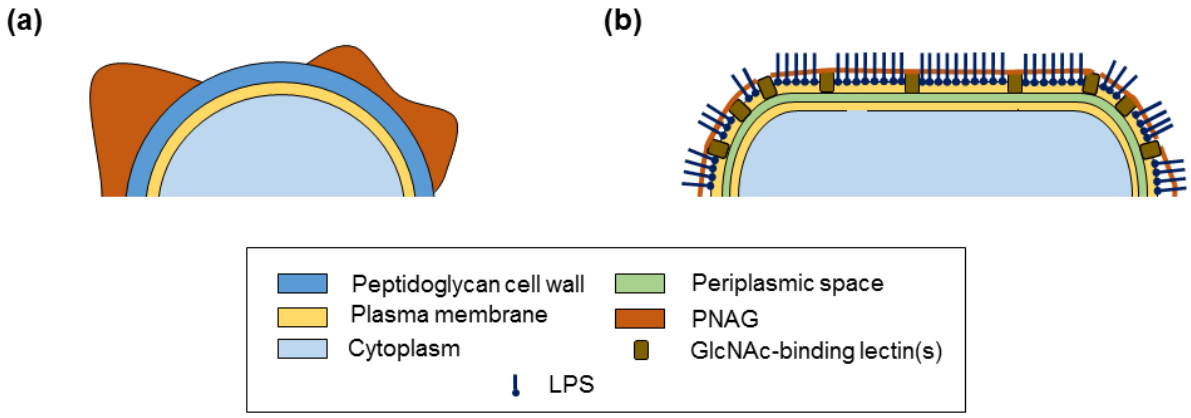

Figure 6. Model of proposed presentation of PNAG on the surface of (**a**) methicillin-sensistive *S. aureus* and (**b**) *A. baumannii*.

In summary, this work showed that sWGA and WGA bind to PNAG in a carbohydrate-dependent manner, that the main surface component of MSSA strain Mn8m was PNAG while for MSSA strain 8325-4 PNAG only partially covered the surface, and that PNAG was not the main accessible surface molecule on *A. baumannii*. This study is also the first to report specific carbohydrate ligands for whole *S. aureus* and *A. baumannii* bacteria, and a GlcNAc-binding lectin function was shown to have a role in PNAG surface presentation or biofilm assembly for *A. baumannii*. Together these data indicated that PNAG surface presentation and accessibility differed between these Gram-negative and Gram-positive species, and that PNAG affected the presentation and accessibility of other surface molecules on *A. baumannii* cells. Based on these data we suggest that PNAG may fulfil different biological and/or physical roles depending on the surface presentation. These findings will help to advance our understanding of host-pathogen interactions, biofilm assembly and mechanisms of pathogenesis.

MATERIALS AND METHODS

The Supplementary Materials can contain details about materials and additional details about the assay for LTA on bacterial cell surface, fluorescent labelling of bacteria, lectin and carbohydrate microarray construction, microarray incubation and scanning.

Materials and bacterial strains used. Agar, Alexa Fluor® 555 (AF555) carboxylic acid succinimidyl ester fluorescent label, Pierce™ enchanced chemiluminescence (ECL) Western blotting substrate, mouse anti-LTA IgG monoclonal antibody (mAb), mouse anti-peptidoglycan IgG1 mAb (3F6B3 (10H6)), Nunc™ MicroWell™ (Nunclon (Δ surface) tissue culture-treated) 96-well microtitre plates and SYTO™ 82 nucleic acid stain was purchased from ThermoFisher Scientific (Dublin, Ireland). The Δ certification is a proprietary cell culture surface treatment that offers maximum adhesion for a broad range of cell types and is used for biofilm assays. Brain Heart Infusion (BHI) agar and crystal violet were obtained from Sigma-Aldrich Co. (Dublin, Ireland). Proteinase K was from QIAGEN (Hilden, Germany). Casein was purchased from BDH, Merck (Dublin, Ireland). Nexterion® Slide H microarray slides were supplied by Schott AG (Mainz, Germany). The DAKO rabbit anti-human IgG antibody (Ab) conjugated to horse radish peroxidase (HRP) and goat anti-mouse Ig-HRP Ab was from Agilent Technologies Ireland, Ltd. (Cork, Ireland). Immoblion-P 0.45 µm polyvinylidene difluoride (PVDF) membrane was from Merck Millipore (Cork, Ireland). Purified LTA from *S. aureus* was purchased from InvivoGen (Toulouse, France). Pure, unlabelled lectins were purchased from EY Labs (San Mateo, CA, U.S.A.) or Vector Laboratories Inc. (Burlingame, CA, U.S.A.) Neoglycoconjugates (NGCs) were purchased from Dextra Laboratories Ltd.(Reading, U.K.) and IsoSep AB (Tullinge, Sweden) or synthesised in house [65] (Tables S3 and S4). Anti-PNAG monoclonal antibody (mAb) (F598) was as previously generated in the Pier lab [66]. All other reagents were purchased from Sigma-Aldrich Co. unless otherwise stated and were of the highest grade available.

Bacterial strains and culture. The *S. aureus* and *A. baumannii* strains used in this study (Table 1) are detailed in Table S1. All bacteria were grown on BHI agar. Agar was supplemented with tetracycline (5 µg/mL) for all *S. aureus* Δ*ica* strains. Bacteria were grown overnight (17 h) in 5 mL cultures at 37 °C with shaking at 180 rpm in BHI, BHI supplemented with 1% (w/v) glucose (BHI glucose) or BHI supplemented with 4% (w/v) NaCl (BHI NaCl) where indicated.

Biofilm assays. Overnight cultures grown in BHI media were adjusted with BHI media to an absorbance at 595 nm of 1.0 and diluted 1:200 with BHI, BHI glucose or BHI NaCl. After mixing, 100 µL was placed in each well of Nunclon (Δ surface) tissue culture-treated 96-well microtitre plates in triplicate per sample, incubated at 37 °C for 24 h, washed three times in a

basin of deionised water and dried at 80 °C for up to 2 h. Crystal violet solution (0.4% (w/v) crystal violet in distilled water, 100 µL) was added to each well and incubated for 5 min at room temperature. The wells were then washed three times with sterile water and 100 µL of 5% (v/v) acetic acid was added to the wells. Absorbance was measured at 490 nm on a SpectraMax M5e microplate reader (Molecular Devices, Inc.). Experiments were carried out in triplicate and the average absorbance and standard error was calculated using Excel v.2010 (Microsoft). To assess biofilm formation by *A. baumannii*, bacteria were grown overnight in BHI media at 37 °C with shaking at 180 rpm. Overnight cultures were diluted 1:200 in BHI glucose in 10 mL borosilicate glass culture tubes in a total volume of 2 mL. Cultures were incubated at 37 °C for 5 h with shaking at 270 rpm, then removed from the tubes and the tubes were washed three times with PBS and dried at 80 °C for 3 h. Crystal violet solution (3 mL) was added to the tubes for 10 min, then washed three times in water, dried at 80 °C for 3 h and the stained tubes imaged using a digital camera. Digital images were stored as .tif files.

Fluorescent labelling of bacteria. Bacterial labelling was carried out in the dark essentially as previously described [20] with some minor alterations. After overnight culture, bacteria were pelleted by centrifugation (5,000 × g, 5 min), washed three times in in Tris-buffered saline supplemented with Ca^{2+} and Mg^{2+} ions (TBS; 20 mM Tris-HCl, 100 mM NaCl, 1 mM $CaCl_2$, 1 mM $MgCl_2$, pH 7.2) and resuspended in 5 mL TBS. Bacteria were diluted with TBS to an absorbance at 595 nm of approximately 1.0. To determine the optimum dye concentration, each bacterial strain was incubated in the dark with a range of 5 to 50 µM SYTO® 82 at 37 °C for 1 h with 180 rpm rotation. Following incubation, the fluorescently labelled cells were washed three times in TBS by resuspending bacteria in 1 mL TBS, centrifuging to pellet at 5,000 x g for 5 min and removing the supernatant to remove excess dye. Bacterial cells were finally resuspended to an approximate absorbance at 595 nm of 2.0 in 0.5 mL of TBS supplemented with 0.025% Tween-20 (TBS-T) and fluorescence was measured (λ_{ex} 541 nm, λ_{em} 560 nm) in a black microtitre plate using a SpectraMax M5e microplate reader (Figure S6). The optimum dye concentration was determined based on maximum fluorescence intensity obtained for the strain (5 µM SYTO® 82 for *S. aureus* Mn8m and Δ*ica* mutant and *A. baumannii* WT and Δ*pga* mutant, and 10 µM for *S. aureus* 8325-4 WT and Δ*ica* mutant). For *S. aureus* BH1CC WT and Δ*ica* mutant, optimum dye concentration of 15 µM was selected based on optimum signal to noise ratio on the lectin microarray (Figure S7).

Assay for PNAG on bacterial cell surface. Bacteria were grown overnight on BHI agar, inoculated in 5 mL of BHI glucose (*S. aureus* Mn8m and *A. baumannii*) or BHI NaCl (*S. aureus* 8325-4 and BH1CC) and grown overnight at 37 °C. Bacterial cells were washed by centrifugation at 5,000 x g for 5 min, resuspending the pellet with sterile TBS to an absorbance at 595 nm of approximately 1.0 (approximately 8 x 10^8 cells/mL) in endotoxin-free water. Cells were killed by heating to 95 °C for 40 min. Heat-killed bacteria were then streaked on BHI agar plates and incubated overnight at 37 °C to confirm cell death by lack of growth. PVDF membrane (0.45 µm) was pre-treated for 15 s in methanol, soaked in TBS for 5 min and allowed to partially dry. PNAG (2 µL of 1 mg/mL) purified from *S. aureus* Mn8m (see below) and heat killed bacteria (2 µL) were pipetted on to the activated membrane in triplicate and allowed to dry. Membranes were then incubated for 1 h in 5% (w/v) skimmed milk in TBS at room temperature, solution was drawn off and human IgG1 anti-PNAG mAb (F598 [66]) (800 µg/mL diluted in TBS 0.0001% Tween® 20, 1% skimmed milk) was added to the membrane and incubated for 1 h. The membrane was then washed three times for 5 min each in TBS 0.0001% Tween® 20 and once in TBS for 5 min. Horseradish peroxidase- (HRP-)conjugated rabbit anti-human IgG antibody (200 µg/mL TBS with 0.0001% Tween® 20 and 1% skimmed milk) was applied to the membrane, incubated at room temperature for 1 h and the membrane washed as above. For development, a chemiluminescent substrate for the detection of HRP activity (Pierce™ ECL Western blotting substrate) was added to the membrane for 1 min before visualisation using a chemiluminescent camera (Alpha Innotech FluorChem FC2 Imaging System). Images were stored digitally as .tif files.

Purification and characterisation of PNAG from *S. aureus* Mn8m. PNAG was purified from 16 L of the PNAG-overproducer *S. aureus* Mn8m culture by ethanol precipitation, enzymatic digestions followed by size exclusion chromatography essentially as previously described [39]. 1D ^{1}H NMR spectra were acquired, also essentially as previously described [39]. For the detection of LTA and peptidoglycan in PNAG, a dot blot was carried out as described above except 2 µL of 1 mg/mL PNAG *S. aureus* Mn8m and 2 µL dilutions of purified LTA purified from *S. aureus* (SA-LTA) were spotted on to the activated PVDF membrane. For a positive peptidoglycan sample, 2 µL of heat killed *S. aureus* Mn8m (8 x 10^8 cells/mL) was spotted on the membrane as a positive control. The membrane was blocked as described above and incubated with anti-LTA mAb (1:50 dilution in TBS-T 0.001%, 1% skimmed-milk) or

mouse IgG1 anti-peptidoglycan mAb (1:50 dilution in TBS with 0.0001% Tween® 20 and 1% skimmed milk) for 1 h at room temperature. The membrane was then washed three times for 5 min each in TBS 0.0001% Tween® 20 and once in TBS for 5 min followed by incubation with HRP-labelled goat anti-mouse IgG antibody (200 µg/mL in TBS-T 0.001%, 1% skimmed-milk) for 1 h at room temperature. The membrane was washed three times in TBS-T and finally in TBS for 5 min. HRP activity was detected as described above and the image was quantified by densitometry using ImageJ and comparing to the standard curve generated by known concentrations of SA-LTA.

Fluorescent labelling of PNAG. The entire procedure was carried out in the dark. PNAG was initially solubilised at 4 mg/mL in 5 M HCl and pH was immediately adjusted to 7.0 with 5 M NaOH. The solubilised PNAG was then diluted to 2 mg/mL in 0.1 M sodium borate (final concentration), pH 8.0, and 0.1 mg of AF555 carboxylic acid succinimidyl ester fluorescent label in 10 µL DMSO was added. The mixture was incubated at 25 °C for 2 h in the dark and the AF555-labelled PNAG (PNAG-AF555) was then purified using a 3 kDa MWCO centrifugal filter with three exchanges of 300 µL phosphate buffered saline (PBS), pH 7.4. PBS (100 µL) was then added to the filter retentate and recovered according to manufacturer's instructions. PNAG-AF555 (approximately 5 mg/mL) was not directly quantified after labelling but was titrated for optimal incubation concentration on lectin microarrays as detailed below.

Lectin and carbohydrate microarray construction. Lectin and carbohydrate microarrays were prepared essentially as previously described [20,65] with minor modifications. In brief, a panel of lectins of known specificities were printed at 0.5 mg/mL in PBS, pH 7.4, supplemented with 1 mM of their respective haptentic monosaccharides (Table S2) in replicates of 6 per probe per subarray and eight replicate subarrays per microarray slide. For carbohydrate microarrays, neoglycoconjugates and glycoproteins were printed at 1 mg/mL in PBS across two paired microarrays, A and B, with 15 of the same probes in the same print position to facilitate later data normalisation across the paired microarrays (Tables S3 and S4). Probes (lectins, NGCs and glycoproteins) were printed on Nexterion ® slide H microarray slides using a SciFlexArrayer S3 (Scienion, Berlin, Germany) under constant 60% (+/- 2%) humidity at 20 °C. For each slide, features of approximately 1 nL were printed in replicates of 6 per probe per subarray and eight replicate subarrays per microarray slide. Following printing, slides were

placed in a humidity chamber overnight at room temperature. Slides were then blocked with 100 mM ethanolamine in 50 mM sodium borate, pH 8.0, for 1 h at room temperature. Slides were washed three times with PBS with 0.05% Tween® 20 (PBS-T), and once with PBS. Slides were dried by centrifugation (1,500 rpm, 5 min) and stored at 4 °C sealed with desiccant until use. Validation of lectin printing and retained function on the microarray surface was carried out by incubating one microarray from each batch with a panel of AF555 labelled glycoproteins (fetuin, asialofetuin, invertase, RNase B and alpha-1-acid glycoprotein) and the neoglycoconjugate GlcNAc-BSA (each incubated at 1 µg/mL in TBS-T). Validation of neoglycoconjugate and glycoprotein printing and accessibility of the presented carbohydrates on the microarray surface was done by incubating one microarray from each batch with a panel of TRITC labelled lectins (WGA, MAA, AIA, Con A, PHA-E, GS-II and SBA, each incubated at 5 µg/mL).

Microarray incubation and scanning. All microarray incubations were carried out in the dark. Labelled bacteria, PNAG, lectins or glycoproteins diluted in TBS-T were incubated on lectin or carbohydrate microarrays essentially as previously described [20] at 70 uL per well and incubated with gentle rotation (4 rpm) at 37 °C for 1 h. Incubation chambers were disassembled under TBS-T, washed twice in TBS-T for 2 min each wash in a Coplin jar and once with TBS. Microarray slides were dried by centrifugation (1,500 rpm, 5 min) and imaged immediately after incubation and washing by scanning in an Agilent G2505B microarray scanner equipped with a 543 nm laser (90% PMT, 5 µm resolution). Images were stored digitally as .tif files (Figure S12). Experiments were carried out in technical triplicate with sample incubation on one microarray slide considered one experimental replicate. All bacterial strains were initially titrated on each microarray platform by incubating dilutions of stained bacteria at absorbance at 595 nm of 2.0 with TBS-T in a final 70 uL per well volume. As *S. aureus* BH1CC had the lowest fluorescence following staining compared to the other *S. aureus* strains and *A. baumannii*, the optimal dilution of 50 µL to a final volume of 70 µL with TBS-T of *S. aureus* BH1CC WT (maximal signal intensity with low background) was selected for use as the dilution for all bacterial strains for consistency (1.1×10^9 cells/mL). For PNAG-AF555 the optimal dilution of 0.2 µL stock per mL of TBS-T was used. For inhibition assays, varying concentrations of the sugar were co-incubated with PNAG-AF555 in different subarrays and compared to uninhibited binding on the same microarray slide.

Data extraction and analysis. Data extraction was performed essentially as previously described [20,50]. Local background subtracted median feature intensity data (F543median-B543) was analysed and the median of six replicate spots per subarray was handled as a single data point for graphical and statistical analysis. For lectin microarray analysis, data were normalized to the per subarray mean total intensity value of three replicate microarray slides and binding data was presented as a bar chart of average intensity of three experimental replicates with error bars of +/- 1 SD of the mean. For carbohydrate microarray analysis, the same process was carried out as for lectin microarray analysis, except that total per subarray intensity was normalised to the common 15 probes across the paired A and B microarrays [50]. IC_{50} values were generated using GraphPad Prism v.8.3.1 (GraphPad Software, San Diego, CA, U.S.A.) using a nonlinear fit of percentage inhibition versus Log_{10} inhibitor concentration. Unsupervised hierarchical clustering of binding data was carried out using Hierarchial Clustering Explorer v3.0 (http://www.cs.umd.edu/hcil/hce/hce3.html; National Institutes of Health, Bethesda, MD, U.S.A.). Normalised microarray data was scaled to the maximum signal intensity per sample and the binding patterns were clustered using no pre-filtering, complete linkage and Euclidean distance. T-tests comparing mutant and WT binding were carried out using normalised data, 2 tailed and unequal variance.

ASSOCIATED CONTENT

Supporting information

The Supporting Information is available free of charge on the ACS Publications website at DOI:

AUTHOR INFORMATION

ORCID

Gerald B. Pier: 0000-0002-9112-2331

James P. O'Gara: 0000-0003-3866-7161

Michelle Kilcoyne: 0000-0002-8870-1308

Author contributions

A.F. carried out all experiments, A.F. and M.K. conceptualised the work and wrote the manuscript, A.F., M.L.B. and M.K. performed the analysis, M.K. supervised the work, and all authors contributed intellectually to the work, writing the manuscript and approved the final manuscript.

Notes

Gerald B. Pier is an inventor of intellectual properties (human monoclonal antibody to PNAG and PNAG vaccines) that are licensed by Brigham and Women's Hospital to Alopexx Vaccine, LLC, and Alopexx Pharmaceuticals, LLC, entities in which Gerald B. Pier also holds equity. As an inventor of intellectual properties, Gerald B. Pier also has the right to receive a share of licensing-related income (royalties, fees) through Brigham and Women's Hospital from Alopexx Pharmaceuticals, LLC, and Alopexx Vaccine, LLC. Gerald B. Pier's interests were reviewed and are managed by the Brigham and Women's Hospital and Partners Healthcare in accordance with their conflict of interest policies. The other authors declare no competing financial interests. The funders had no role in the design of the study; in the collection, analyses, or interpretation of data; in the writing of the manuscript, or in the decision to publish the results.

ACKNOWLEDGEMENTS

We thank the Irish Research Council for the Government of Ireland Postgraduate Scholarship award (AF), the Royal Society of Chemistry Analytical Chemistry Trust Fund (ACTF) for the 2018 ACTF Fellowship award (MK) and the Health Research Board (HRA-POR-2015-1158, JO'G).

REFERENCES

1. Davies, D. Understanding biofilm resistance to antibacterial agents. *Nat. Revs Drug Discov.* **2003**, *2*, 114-122.
2. Khatoon, Z.; McTiernan, C.D.; Suuronen, E.J.; Mah, T.-F.; Alarcon, E.I. Bacterial biofilm formation on implantable devices and approaches to its treatment and prevention. *Heliyon* **2018**, *4*, e01067.

3. World Health Organisation. *Report on the burden of endemic health care-associated infection worldwide*; World Health Organisation: Geneva, Switzerland, 2011.
4. Santajit, S.; Indrawattana, N. Mechanisms of antimicrobial resistance in ESKAPEpathogens. *BioMed Res. Int.* **2016**, *2016*, 8.
5. Lin, M.H.; Shu, J.C.; Lin, L.P.; Chong, K.y.; Cheng, Y.W.; Du, J.F.; Liu, S.-T. Elucidating the crucial role of poly *n*-acetylglucosamine from *Staphylococcus aureus* in cellular adhesion and pathogenesis. *PLOS ONE* **2015**, *10*, e0124216.
6. Maira-Litran, T.; Kropec, A.; Goldmann, D.; Pier, G.B. Biologic properties and vaccine potential of the staphylococcal poly-*N*-acetylglucosamine surface polysaccharide. *Vaccine* **2004**, *22*, 872-879.
7. Wang, Y.-C.; Huang, T.-W.; Yang, Y.-S.; Kuo, S.-C.; Chen, C.-T.; Liu, C.-P.; Liu, Y.-M.; Chen, T.-L.; Chang, F.-Y.; Wu, S.-H.*, et al.* Biofilm formation is not associated with worse outcome in *Acinetobacter baumannii* bacteraemic pneumonia. *Sci. Rep.* **2018**, *8*, 7289.
8. O'Neill, E.; Pozzi, C.; Houston, P.; Smyth, D.; Humphreys, H.; Robinson, D.A.; O'Gara, J.P. Association between methicillin susceptibility and biofilm regulation in *Staphylococcus aureus* isolates from device-related infections. *J. Clin. Microbiol.* **2007**, *45*, 1379-1388.
9. Pozzi, C.; Waters, E.M.; Rudkin, J.K.; Schaeffer, C.R.; Lohan, A.J.; Tong, P.; Loftus, B.J.; Pier, G.B.; Fey, P.D.; Massey, R.C.*, et al.* Methicillin resistance alters the biofilm phenotype and attenuates virulence in *Staphylococcus aureus* device-associated infections. *PLOS Pathog.* **2012**, *8*, e1002626.
10. Vuong, C.; Kocianova, S.; Voyich, J.M.; Yao, Y.; Fischer, E.R.; DeLeo, F.R.; Otto, M. A crucial role for exopolysaccharide modification in bacterial biofilm formation, immune evasion, and virulence. *J. Biol. Chem.* **2004**, *279*, 54881-54886.
11. Cerca, N.; Jefferson, K.K. Effect of growth conditions on poly-*N*-acetylglucosamine expression and biofilm formation in *Escherichia coli*. *FEMS Microbiol. Letts* **2008**, *283*, 36-41.
12. Conlon, K.M.; Humphreys, H.; O'Gara, J.P. *Icar* encodes a transcriptional repressor involved in environmental regulation of *ica* operon expression and biofilm formation in *Staphylococcus epidermidis*. *J. Bacteriol.* **2002**, *184*, 4400-4408.
13. Götz, F. Staphylococcus and biofilms. *Mol. Microbiol.* **2002**, *43*, 1367-1378.
14. Muñoz, A.; Alvarez, O.; Alonsa, B.; Llovo, J. Lectin typing of methicillin-resistant *Staphylococcus aureus*. *J. Med. Microbiol.* **1999**, *48*, 495-499.
15. Neu, R.T.; Kuhlicke, U. Fluorescence lectin bar-coding of glycoconjugates in the extracellular matrix of biofilm and bioaggregate forming microorganisms. *Microorganisms* **2017**, *5*.
16. Khan, M.M.; Ernst, O.; Manes, N.P.; Oyler, B.L.; Fraser, I.D.C.; Goodlett, D.R.; Nita-Lazar, A. Multi-omics strategies uncover host–pathogen interactions. *ACS Inf. Dis.* **2019**, *5*, 493-505.
17. Fong, J.N.C.; Yildiz, F.H. Biofilm matrix proteins. *Microbiol. Spectr.* **2015**, *3*.
18. Passos da Silva, D.; Matwichuk, M.L.; Townsend, D.O.; Reichhardt, C.; Lamba, D.; Wozniak, D.J.; Parsek, M.R. The *Pseudomonas aeruginosa* lectin lecb binds to the exopolysaccharide psl and stabilizes the biofilm matrix. *Nat. Commun.* **2019**, *10*, 2183.
19. Hsu, K.-L.; Pilobello, K.T.; Mahal, L.K. Analyzing the dynamic bacterial glycome with a lectin microarray approach. *Nat. Chem. Biol.* **2006**, *2*, 153-157.
20. Kilcoyne, M.; Twomey, M.E.; Gerlach, J.Q.; Kane, M.; Moran, A.P.; Joshi, L. *Campylobacter jejuni* strain discrimination and temperature-dependent glycome expression profiling by lectin microarray. *Carbohydr. Res.* **2014**, *389*, 123-133.
21. Yasuda, E.; Tateno, H.; Hirabarashi, J.; Iino, T.; Sako, T. Lectin microarray reveals binding profiles of *lactobacillus casei* strains in a comprehensive analysis of bacterial cell wall polysaccharides. *Appl. Environ. Microbiol.* **2011**, *77*, 4539-4546.
22. Flannery, A.; Gerlach, J.Q.; Joshi, L.; Kilcoyne, M. Assessing bacterial interactions using carbohydrate-based microarrays. *Microarrays* **2015**, *4*, 690-713.

23. Horsburgh, M.J.; Aish, J.L.; White, I.J.; Shaw, L.; Lithgow, J.K.; Foster, S.J. Σ^b modulates virulence determinant expression and stress resistance: Characterization of a functional *rsbu* strain derived from *Staphylococcus aureus* 8325-4. *J. Bacteriol.* **2002**, *184*, 5457-5467.
24. McKenney, D.; Pouliot, K.L.; Wang, Y.; Murthy, V.; Ulrich, M.; Döring, G.; Lee, J.C.; Goldmann, D.A.; Pier, G.B. Broadly protective vaccine for *Staphylococcus aureus* based on an *in vivo*-expressed antigen. *Science* **1999**, *284*, 1523-1527.
25. Jefferson, K.K.; Cramton, S.E.; Götz, F.; Pier, G.B. Identification of a 5-nucleotide sequence that controls expression of the ica locus in *Staphylococcus aureus* and characterization of the DNA-binding properties of icar. *Mol. Microbiol.* **2003**, *48*, 889-899.
26. Fitzpatrick, F.; Humphreys, H.; O'Gara, J.P. Evidence for *icaadbc*-independent biofilm development mechanism in methicillin-resistant *Staphylococcus aureus* clinical isolates. *J. Clin. Microbiol.* **2005**, *43*, 1973-1976.
27. Houston, P.; Rowe, S.E.; Pozzi, C.; Waters, E.M.; O'Gara, J.P. Essential role for the major autolysin in the fibronectin-binding protein-mediated *Staphylococcus aureus* biofilm phenotype. *Infect. Immun.* **2011**, *79*, 1153-1165.
28. Choi, A.H.K.; Slamti, L.; Avci, F.Y.; Pier, G.B.; Maira-Litrán, T. The *pgaabcd* locus of *Acinetobacter baumannii* encodes the production of poly-β-1-6-*N*-acetylglucosamine, which is critical for biofilm formation. *J. Bacteriol.* **2009**, *191*, 5953-5963.
29. Kennedy, C.A.; O' Gara, J.P. Contribution of culture media and chemical properties of polystyrene tissue culture plates to biofilm development by *Staphylococcus aureus*. *J. Med. Microbiol.* **2004**, *53*, 1171-1173.
30. Lim, Y.; Jana, M.; Luong, T.T.; Lee, C.Y. Control of glucose- and nacl-induced biofilm formation by *rbf* in *Staphylococcus aureus*. *J. Bacteriol.* **2004**, *186*, 722-729.
31. Jefferson, K.K.; Pier, D.B.; Goldmann, D.A.; Pier, G.B. The teicoplanin-associated locus regulator (tcar) and the intercellular adhesin locus regulator (icar) are transcriptional inhibitors of the *ica* locus in *Staphylococcus aureus*. *J. Bacteriol.* **2004**, *186*, 2449-2456.
32. Whitfield, G.B.; Marmont, L.S.; Howell, P.L. Enzymatic modifications of exopolysaccharides enhance bacterial persistence. *Front. Microbiol.* **2015**, *6*.
33. Formosa-Dague, C.; Feuillie, C.; Beaussart, A.; Derclaye, S.; Kucharíková, S.; Lasa, I.; Van Dijck, P.; Dufrêne, Y.F. Sticky matrix: Adhesion mechanism of the staphylococcal polysaccharide intercellular adhesin. *ACS Nano* **2016**, *10*, 3443-3452.
34. Sanford, B.A.; Thomas, V.L.; Mattingly, S.J.; Ramsay, M.A.; Miller, M.M. Lectin-biotin assay for slime present in *in situ* biofilm produced by *Staphylococcus epidermidis* using transmission electron microscopy (TEM). *J. Ind. Microbiol.* **1995**, *15*, 156-161.
35. Begun, J.; Gaiani, J.M.; Rohde, H.; Mack, D.; Calderwood, S.B.; Ausubel, F.M.; Sifri, C.D. Staphylococcal biofilm exopolysaccharide protects against *Caenorhabditis elegans* immune defenses. *PLOS Pathog.* **2007**, *3*, e57.
36. Ramos, Y.; Rocha, J.; Hael, A.L.; van Gestel, J.; Vlamakis, H.; Cywes-Bentley, C.; Cubillos-Ruiz, J.R.; Pier, G.B.; Gilmore, M.S.; Kolter, R.*, et al.* PolyGlcNAc-containing exopolymers enable surface penetration by non-motile *Enterococcus faecalis*. *PLOS Pathog.* **2019**, *15*, e1007571.
37. Cerca, N.; Jefferson, K.K.; Oliveira, R.; Pier, G.B.; Azeredo, J. Comparative antibody-mediated phagocytosis of *Staphylococcus epidermidis* cells grown in a biofilm or in the planktonic state. *Infect. Immun.* **2006**, *74*, 4849-4855.
38. Sizemore, R.K.; Caldwell, J.J.; Kendrick, A.S. Alternate Gram staining technique using a fluorescent lectin. *Appl. Environ. Microbiol.* **1990**, *56*, 2245-2247.
39. Maira-Litrán, T.; Kropec, A.; Abeygunawardana, C.; Joyce, J.; Mark, G.; Goldmann, D.A.; Pier, G.B. Immunochemical properties of the staphylococcal poly-*N*-acetylglucosamine surface polysaccharide. *Infect. Immun.* **2002**, *70*, 4433-4440.

40. Ginsburg, I. Role of lipoteichoic acid in infection and inflammation. *Lancet Infect. Dis.* **2002**, *2*, 171-179.
41. Duckworth, M.; Archibald, A.R.; Baddiley, J. Lipoteichoic acid and lipoteichoic acid carrier in *Staphylococcus aureus* H. *FEBS Letts* **1975**, *53*, 176-179.
42. Vinogradov, E.; Sadovskaya, I.; Li, J.; Jabbouri, S. Structural elucidation of the extracellular and cell-wall teichoic acids of *Staphylococcus aureus* Mn8m, a biofilm forming strain. *Carbohydr. Res.* **2006**, *341*, 738-743.
43. O'Neill, E.; Pozzi, C.; Houston, P.; Humphreys, H.; Robinson, D.A.; Loughman, A.; Foster, T.J.; O'Gara, J.P. A novel *Staphylococcus aureus* biofilm phenotype mediated by the fibronectin-binding proteins, Fnbpa and Fnbpb. *J. Bacteriol.* **2008**, *190*, 3835-3850.
44. Bæk, K.T.; Gründling, A.; Mogensen, R.G.; Thøgersen, L.; Petersen, A.; Paulander, W.; Frees, D. B-lactam resistance in methicillin-resistant *Staphylococcus aureus* USA300 is increased by inactivation of the clpxp protease. *Antimicrob. Agents Chemother.* **2014**, *58*, 4593-4603.
45. Kawai, M.; Yamada, S.; Ishidoshiro, A.; Oyamada, Y.; Ito, H.; Yamagishi, J.-i. Cell-wall thickness: Possible mechanism of acriflavine resistance in meticillin-resistant *Staphylococcus aureus*. *J. Med. Microbiol.* **2009**, *58*, 331-336.
46. Liang, C.-H.; Wang, S.-K.; Lin, C.-W.; Wang, C.-C.; Wong, C.-H.; Wu, C.-Y. Effects of neighboring glycans on antibody-carbohydrate interaction. *Angew. Chem. Int. Ed.* **2011**, *50*, 1608-1612.
47. Otto, M. Staphylococcal biofilms. *Microbiol. Spectr.* **2018**, *6*.
48. Arbatsky, N.P.; Shneider, M.M.; Kenyon, J.J.; Shashkov, A.S.; Popova, A.V.; Miroshnikov, K.A.; Volozhantsev, N.V.; Knirel, Y.A. Structure of the neutral capsular polysaccharide of *Acinetobacter baumannii* NIPH146 that carries the kl37 capsule gene cluster. *Carbohydr. Res.* **2015**, *413*, 12-15.
49. MacLean, L.L.; Perry, M.B.; Chen, W.; Vinogradov, E. The structure of the polysaccharide O-chain of the LPS from *Acinetobacter baumannii* strain ATCC 17961. *Carbohydr. Res.* **2009**, *344*, 474-478.
50. Utratna, M.; Annuk, H.; Gerlach, J.Q.; Lee, Y.C.; Kane, M.; Kilcoyne, M.; Joshi, L. Rapid screening for specific glycosylation and pathogen interactions on a 78 species avian egg white glycoprotein microarray. *Sci. Rep.* **2017**, *7*, 6477.
51. Iyer, R.N.; Goldstein, I.J. Quantitative studies on the interaction of Concanavalin A, the carbohydrate-binding protein of the jack bean, with model carbohydrate-protein conjugates. *Immunochemistry* **1973**, *10*, 313-322.
52. Oyelaran, O.; Li, Q.; Farnsworth, D.; Gildersleeve, J.C. Microarrays with varying carbohydrate density reveal distinct subpopulations of serum antibodies. *J. Proteome Res.* **2009**, *8*, 3529-3538.
53. Wacklin, P.; Mäkivuokko, H.; Alakulppi, N.; Nikkilä, J.; Tenkanen, H.; Räbinä, J.; Partanen, J.; Aranko, K.; Mättö, J. Secretor genotype (FUT2 gene) is strongly associated with the composition of Bifidobacteria in the human intestine. *PLOS ONE* **2011**, *6*, e20113.
54. Nurjadi, D.; Lependu, J.; Kremsner, P.G.; Zanger, P. *Staphylococcus aureus* throat carriage is associated with ABO-/secretor status. *J. Infect.* **2012**, *65*, 310-317.
55. Saadi, A.T.; Weir, D.M.; Poxton, I.R.; Stewart, J.; Essery, S.D.; Caroline Blackwell, C.; Raza, M.W.; Busuttil, A. Isolation of an adhesin from *Staphylococcus aureus* that binds Lewis blood group antigen and its relevance to sudden infant death syndrome. *FEMS Immunol. Med. Microbiol.* **1994**, *8*, 315-320.
56. Piroth, L.; Que, Y.-A.; Widmer, E.; Panchaud, A.; Piu, S.; Entenza, J.M.; Moreillon, P. The fibrinogen- and fibronectin-binding domains of *Staphylococcus aureus* fibronectin-binding protein a synergistically promote endothelial invasion and experimental endocarditis. *Infect. Immun.* **2008**, *76*, 3824-3831.

57. Hwang, H.S.; Kim, B.S.; Park, H.; Park, H.-Y.; Choi, H.-D.; Kim, H.H. Type and branched pattern of N-glycans and their structural effect on the chicken egg allergen ovotransferrin: A comparison with ovomucoid. *Glycoconjug. J.* **2014**, *31*, 41-50.
58. Ruhaak, L.R.; Koeleman, C.A.M.; Uh, H.-W.; Stam, J.C.; van Heemst, D.; Maier, A.B.; Houwing-Duistermaat, J.J.; Hensbergen, P.J.; Slagboom, P.E.; Deelder, A.M.*, et al.* Targeted biomarker discovery by high throughput glycosylation profiling of human plasma alpha1-antitrypsin and immunoglobulin A. *PLOS ONE* **2013**, *8*, e73082.
59. Dengler, V.; Foulston, L.; DeFrancesco, A.S.; Losick, R. An electrostatic net model for the role of extracellular DNA in biofilm formation by *Staphylococcus aureus*. *J. Bacteriol.* **2015**, *197*, 3779-3787.
60. Gottenbos, B.; Grijpma, D.W.; van der Mei, H.C.; Feijen, J.; Busscher, H.J. Antimicrobial effects of positively charged surfaces on adhering Gram-positive and Gram-negative bacteria. *J. Antimicrob. Chemother.* **2001**, *48*, 7-13.
61. Buist, G.; Steen, A.; Kok, J.; Kuipers, O.P. LysM, a widely distributed protein motif for binding to (peptido)glycans. *Mol. Microbiol.* **2008**, *68*, 838-847.
62. Cabral, M.P.; Soares, N.C.; Aranda, J.; Parreira, J.R.; Rumbo, C.; Poza, M.; Valle, J.; Calamia, V.; Lasa, Í.; Bou, G. Proteomic and functional analyses reveal a unique lifestyle for *Acinetobacter baumannii* biofilms and a key role for histidine metabolism. *J. Proteome Res.* **2011**, *10*, 3399-3417.
63. Vuong, C.; Voyich, J.M.; Fischer, E.R.; Braughton, K.R.; Whitney, A.R.; DeLeo, F.R.; Otto, M. Polysaccharide intercellular adhesin (pia) protects *staphylococcus epidermidis* against major components of the human innate immune system. *Cell. Microbiol.* **2004**, *6*, 269-275.
64. Gaddy, J.A.; Actis, L.A. Regulation of *Acinetobacter baumannii* biofilm formation. *Future Microbiol.* **2009**, *4*, 273-278.
65. Kilcoyne, M.; Gerlach, J.Q.; Kane, M.; Joshi, L. Surface chemistry and linker effects on lectin–carbohydrate recognition for glycan microarrays. *Anal. Methods* **2012**, *4*, 2721-2728.
66. Kelly-Quintos, C.; Cavacini, L.A.; Posner, M.R.; Goldmann, D.; Pier, G.B. Characterization of the opsonic and protective activity against *Staphylococcus aureus* of fully human monoclonal antibodies specific for the bacterial surface polysaccharide poly-*N*-acetylglucosamine. *Infect. Immun.* **2006**, *74*, 2742-2750.

Supplementary information

Glycomics microarrays reveal differential *in situ* presentation of the biofilm polysaccharide poly-*N*-acetylglucosamine on *Acinetobacter baumannii* and *Staphylococcus aureus* cell surfaces

Andrea Flannery,[1,2] Marie Le Berre,[3] Gerald B. Pier,[4] James P. O'Gara,[2] Michelle Kilcoyne[1,3,*]

[1] Carbohydrate Signalling Group, Discipline of Microbiology, National University of Ireland Galway, Galway, Ireland.

[2] Infectious Disease Laboratory, Discipline of Microbiology, National University of Ireland Galway, Galway, Ireland.

[3] Advanced Glycoscience Research Cluster, School of Natural Sciences, National University of Ireland Galway, Galway, Ireland.

[4] Division of Infectious Diseases, Department of Medicine, Brigham and Women's Hospital, Harvard Medical School, Boston, MA, U.S.A.

***** Corresponding author. Email: Michelle.Kilcoyne@nuigalway.ie

Table of contents

Results and Discussion

Bacterial strain selection and verification of biofilm production. The MSSA strains 8325-4 and Mn8m were selected as Gram-positive organisms that produce PNAG-predominant biofilm (Table 1 and Table S1) [1,2]. In *S. aureus*, PNAG is produced by proteins encoded in the *ica* operon and thus the Δ*ica* mutants of the *S. aureus* strains [3,4] were included in this study. The MRSA clinical isolate strain BH1CC has an *ica* operon but does not produce PNAG. Instead eDNA is the main biofilm component [5]. *S. aureus* BH1CC wild type (WT) and the Δ*ica* mutant were included for comparison with the MSSA strains. In some species of Gram-negative bacteria, PNAG is synthesised by proteins produced by the *pga* operon, so the PNAG-producing clinical isolate *A. baumannii* strain S1 WT and its Δ*pga* mutant [6] were also included. Anti-PNAG monoclonal antibody (mAb) was used in a dot blot assay to confirm that the PNAG-producing strains *S. aureus* 8325-4, *S. aureus* Mn8m and *A. baumannii* S1 cultured under biofilm-promoting conditions retained PNAG *in situ* on the cell surface under experimental conditions, while the Δ*ica* and Δ*pga* mutants did not present any PNAG as expected (Figure 1(b)).

It is critical to initially verify that the selected strains and corresponding PNAG-deficient Δ*ica* or Δ*pga* mutants behaved as previously reported, so crystal violet biofilm assays were performed on these strains (Table 1 and Figure S1). All bacterial strains were grown in the presence of 1% glucose supplemented into the growth media (Figure S1) as glucose promotes PNAG-mediated biofilm formation in the MSSA strains but in MRSA clinical isolates, glucose promotes biofilm formation *via* an *ica*-independent mechanism that involves extracellular surface proteins, such as FnBPAB, and eDNA [4,7,8]. Four percent NaCl was also added to the growth media of MRSA BH1CC as it promotes *icaA* transcription but does not promote biofilm formation [7]. As a comparison, the MSSA strain 8325-4 was also grown in the presence of NaCl which increases PNAG-mediated biofilm formation in this strain [9].

Addition of glucose to brain heart infusion (BHI) media increased biofilm formation by *S. aureus* 8325-4 WT by approximately 165% in comparison to *S. aureus* 8325-4 grown in BHI media (Figure S1A) and by 311% with the addition of NaCl to BHI. *S. aureus* 8325-4 Δ*ica* decreased biofilm formation by approximately 73%, 66% and 96% compared to the WT grown in the same media, respectively, which confirmed PNAG-mediated biofilm formation (Figure S1A). *S. aureus* Mn8m WT biofilm was increased slightly (approximately 5%) by the

addition of glucose compared to BHI alone, while *S. aureus* Mn8 Δ*ica* biofilm formation decreased by approximately 92% in BHI and 86% in BHI glucose compared to the WT strain under the same conditions (Figure S1B), which indicated that PNAG was the major contributor to biofilm formation of this MSSA strain. *S. aureus* BH1CC had increased biofilm formation (approximately 62%) when cultured in BHI glucose compared to BHI alone but the addition of NaCl decreased biofilm formation by 90% (Figure S1C). *S. aureus* BH1CC Δ*ica* decreased biofilm formation slightly, by approximately 16%, 13% and 2% of the WT biofilm formed when grown in BHI alone, BHI glucose and BHI NaCl, respectively, but these differences were not significant. This indicated that *S. aureus* BH1CC biofilm formation was not PNAG-dependent. As *A. baumannii* preferentially forms biofilm on glass [6], *A. baumannii* S1 WT and Δ*pga* were grown in the presence of BHI supplemented with 1% Glc in a borosilicate glass culture tube with vigorous shaking (Figure S1D). Crystal violet staining was more intense on the *A. baumannii* S1 WT glass culture tube compared to the Δ*pga* mutant which indicated that while the majority component of *A. baumannii* biofilm was PNAG, other macromolecules (e.g. protein or eDNA) are also components of its biofilm.

Overall, these data confirmed that *S. aureus* strains 8325-4 and Mn8m WT had increased biofilm formation in the presence of glucose and/or NaCl and that this biofilm was primarily composed of PNAG, *S. aureus* BH1CC WT had increased biofilm formation in the presence of glucose and decreased or abolished biofilm in NaCl but PNAG was not involved in biofilm formation as expected and that PNAG contributed to *A. baumannii* S1 biofilm formation.

Surface PNAG retention under experimental conditions. For glycomic microarray analysis it is necessary to fluorescently label bacteria internally by optimising the dye concentrations for each strain under biofilm-promoting conditions (Figures S5–S8). To minimise signal quenching and potential interference of the free highly charged fluorescent molecules in bacterial interactions, the bacteria must be thoroughly washed after staining to remove excess dye [10]. Accordingly several wash conditions after SYTO®82 staining were assessed to determine the retention of PNAG on the bacterial surface (Figure S5). The positive reference of maximal PNAG retention (100%) was for *S. aureus* 8325-4 WT not washed after staining with SYTO® 82 with release of bound PNAG and detection of the released PNAG by anti-PNAG mAb. Washing three times and resuspension of the labelled cells in Tris buffered saline with Ca^{2+} and Mg^{2+} ions (TBS) supplemented with no or varying concentrations of detergent were compared (Figure S5). Although wash buffer with no

detergent retained more cell-surface PNAG compared to wash buffer including detergent (approximately 60% retention), not including detergent in microarray incubations resulted in bacterial clumping. Hence washing the stained bacteria three times and resuspension in TBS supplemented with 0.025% Tween-20 (TBS-T) was selected for all microarray experiments.

Supplementary figures

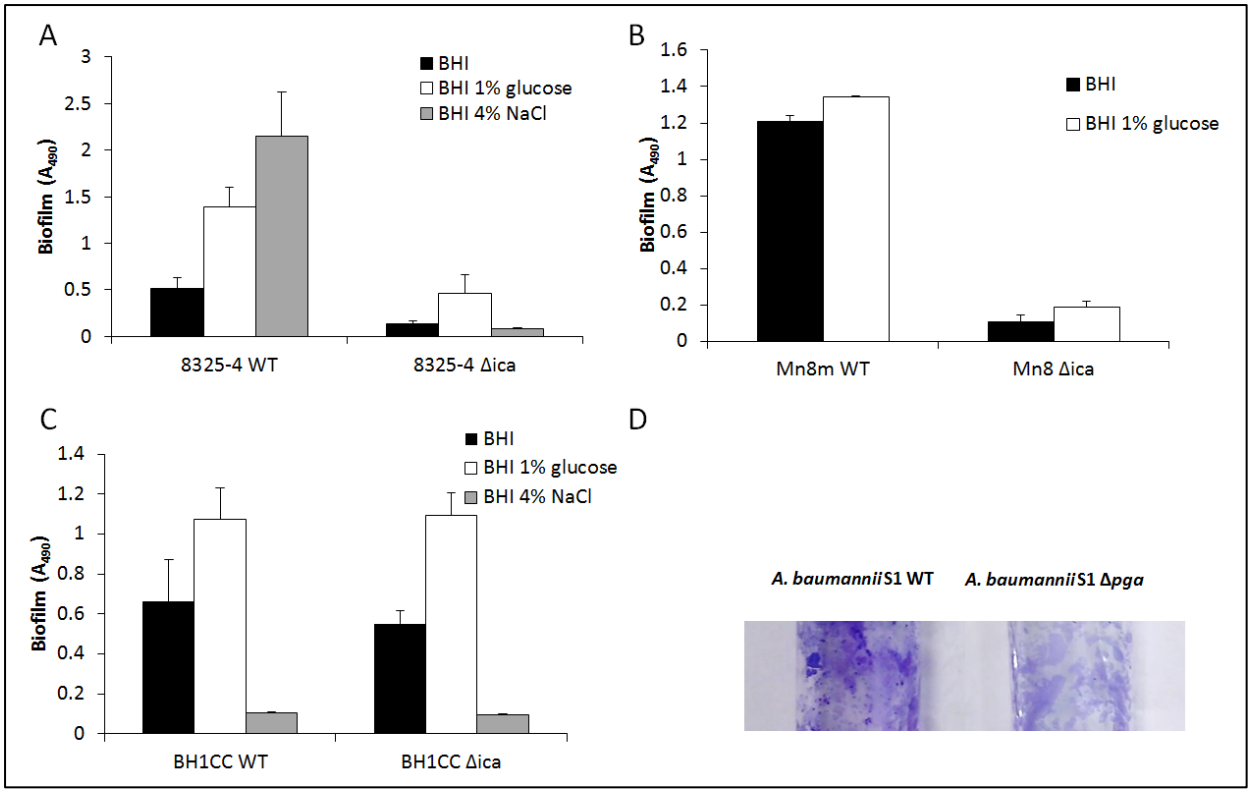

Figure S1. Biofilm assays for (**A**) *S. aureus* 8325-4 wild type (WT) and Δ*ica*, (**B**) *S. aureus* Mn8m WT and Δ*ica*, (**C**) *S. aureus* BH1CC WT and Δ*ica*, and (**D**) *A. baumannii* S1 WT and Δ*pga*. For (**A**), (**B**) and (**C**), bacteria were grown BHI, BHI supplemented with 1% glucose or 4% NaCl in a hydrophilic 96-well tissue culture-treated plate for 18 h. Biofilm was quantified by adding crystal violet and measuring the absorbance at 490 nm. Experiments were carried out in technical triplicates and data is presented as the mean of the three technical replicates of three experiments with error bars of +/- 1 standard deviation (SD) of the mean. (**D**) Bacteria were grown for 18 h in borosilicate glass tubes. Tubes were washed and stained with crystal violet, washed with water, dried and imaged using a camera.

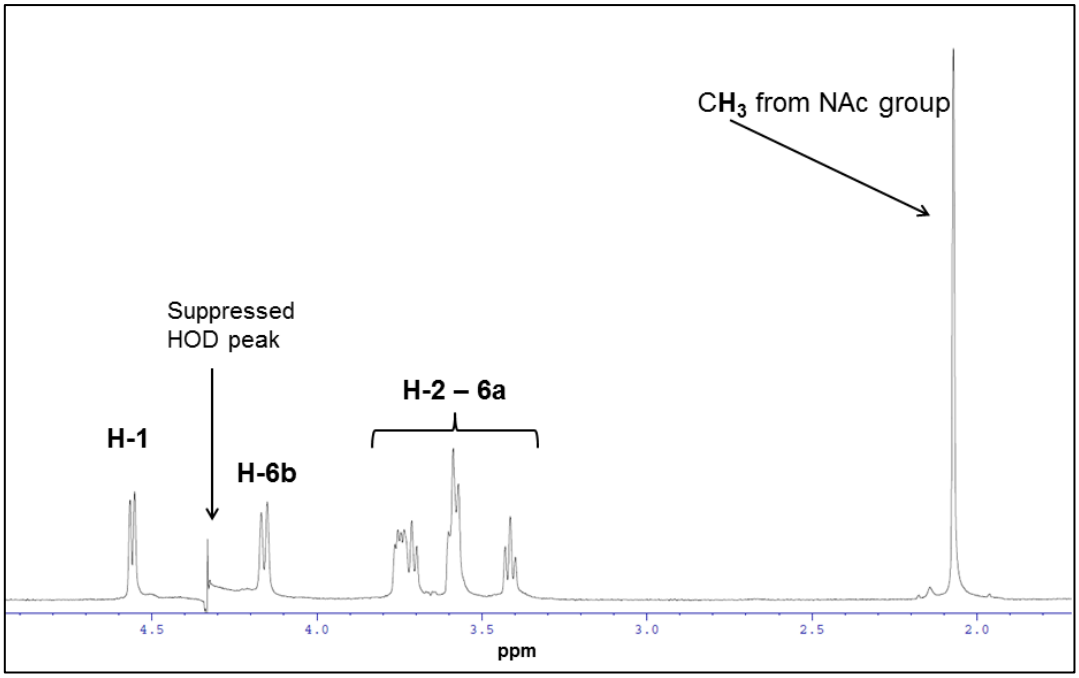

Figure S2. 600 MHz ^{1}H NMR spectra of *S. aureus* Mn8m PNAG in D_2O. Assignments as previously published [11].

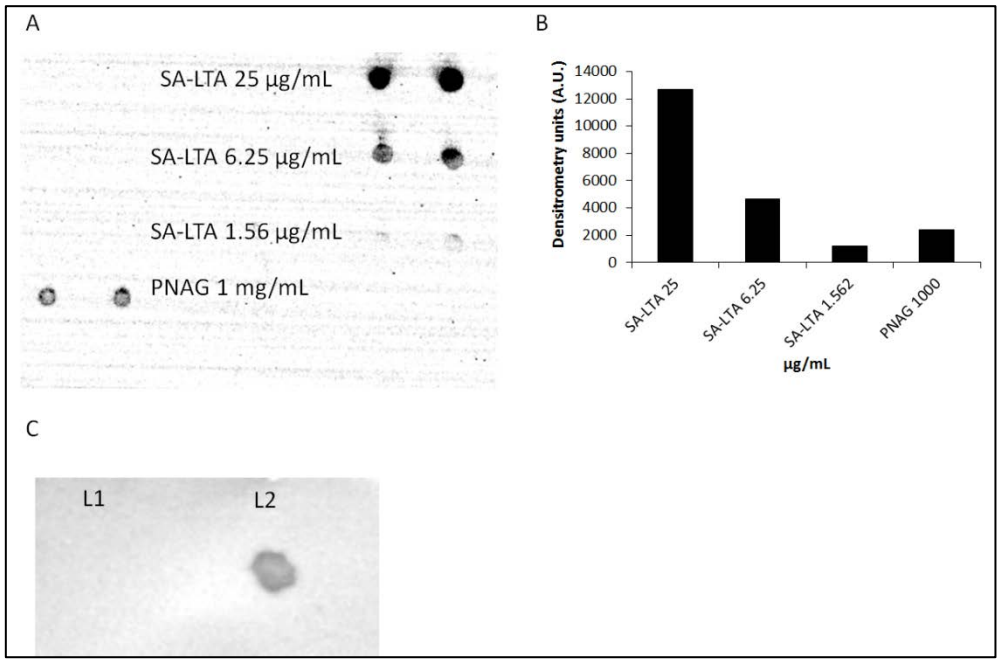

Figure S3. Dot blot assay for the detection of lipoteichoic acid (LTA) and peptidoglycan. (**A**) Dot blot assay of a standard curve of *S. aureus* LTA (SA-LTA) at 25, 6.25 and 1.56 µg/mL and partially purified PNAG (1 mg/mL). Black colour intensity represents anti-LTA antibody (Ab) binding. Spotting was carried out in duplicates. (**B**) Densitometry analysis of image (A) using ImageJ software. (**C**) Dot blot assay for peptidoglycan detection using an anti-peptidoglycan monoclonal Ab. L1 represents the PNAG preparation and L2 represents 8 x 10^8 cells/mL of heat killed *S. aureus.*

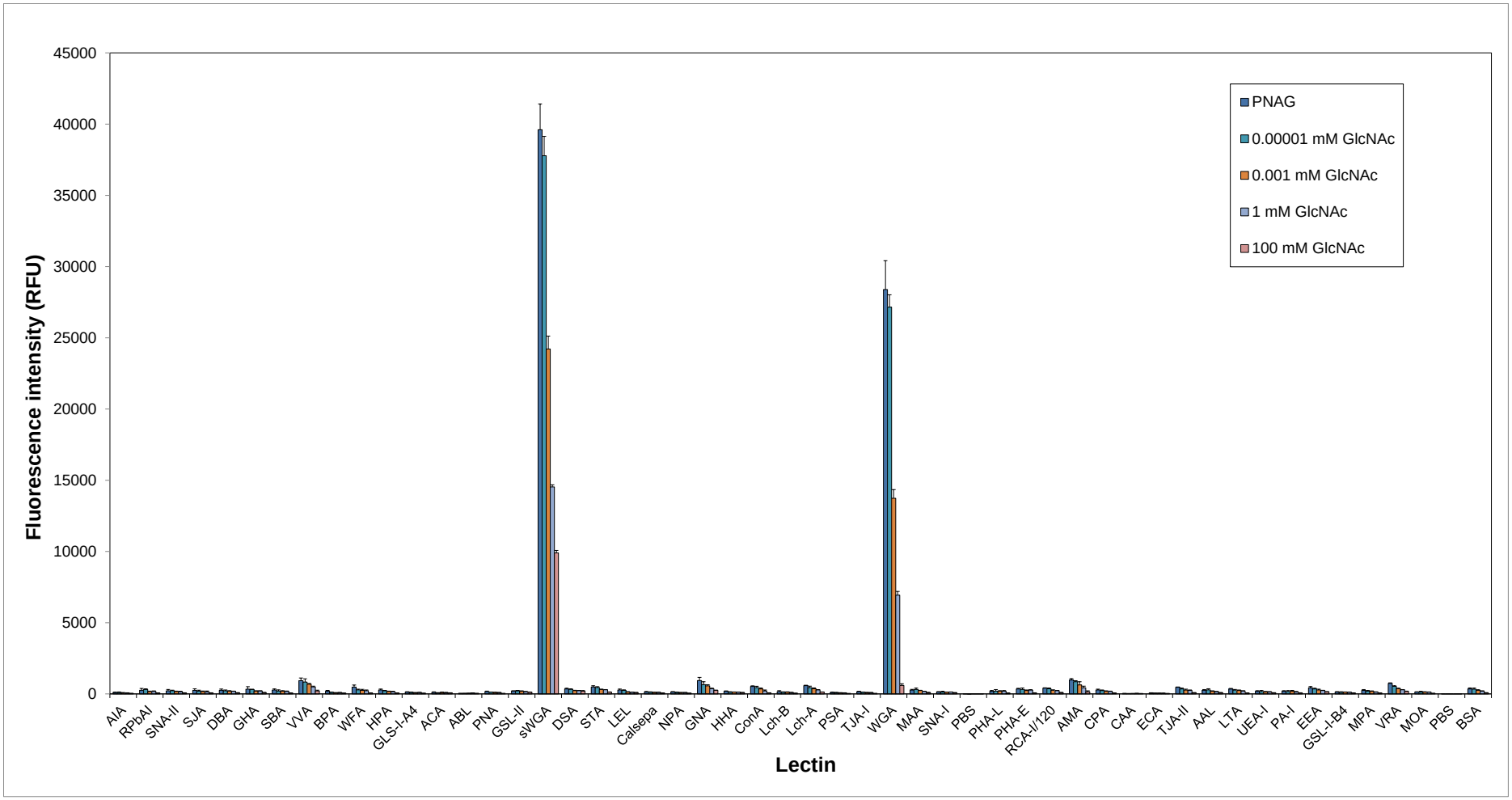

Figure S4. Fluorescently labelled PNAG incubated on the lectin microarray with co-incubation of different concentrations of GlcNAc as indicated in legend. Bars represent the mean of three experiments with error bars of +/- 1 SD of the mean.

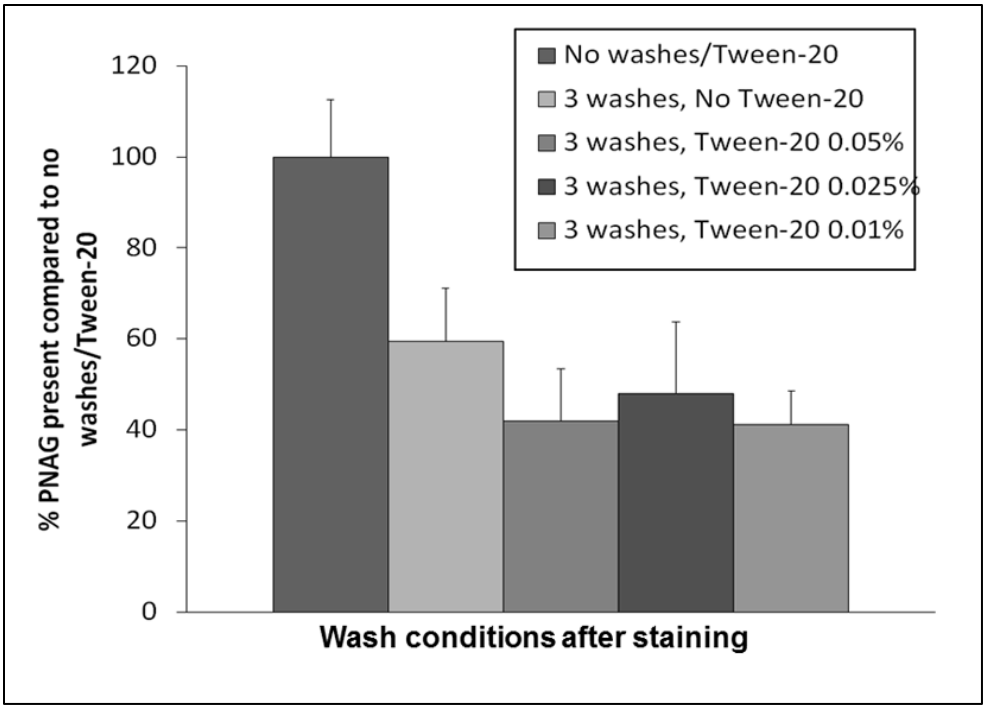

Figure S5. Detection of PNAG released from *S. aureus* 8325-4 WT surface with no washes and after three washes with no and varying Tween-20 concentrations. Anti-PNAG mAb binding was quantified by densitometry and the presence of PNAG was plotted as a relative percentage of no washing after staining (100%).

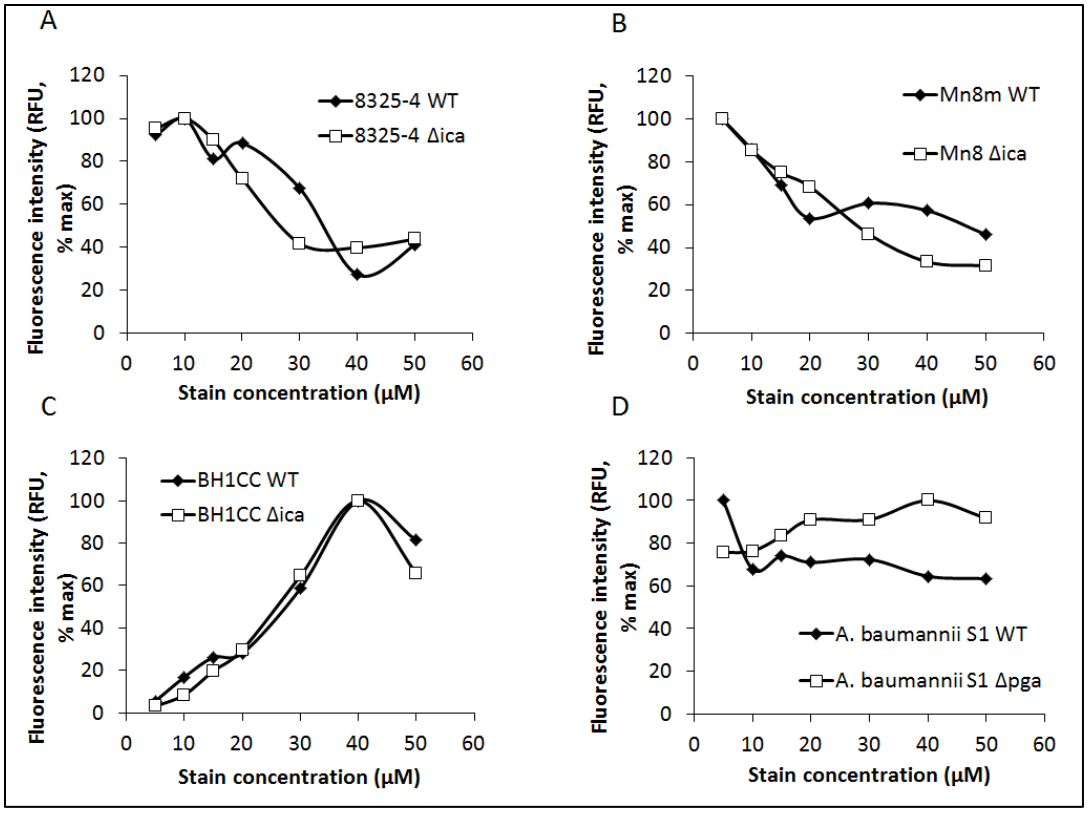

Figure S6. SYTO®82 concentration titration for bacterial fluorescence of (**A**) *S. aureus* 8325-4 WT and Δ*ica*, (**B**) *S. aureus* Mn8m WT and Δ*ica*, (**C**) *S. aureus* BH1CC WT and Δ*ica* and (**D**) *A. baumannii* S1 WT and Δ*pga*. For (**B**), (**C**) and (**D**), bacteria were grown overnight in BHI glucose, while (**A**) *S. aureus* 8325-4 was grown in BHI NaCl, and all strains were incubated with 5-50 μM SYTO®82. Fluorescence of the stained bacteria was measured at λ_{ex} 541 nm and λ_{em} 560 nm and plotted as a percentage of maximum fluorescence obtained for each strain.

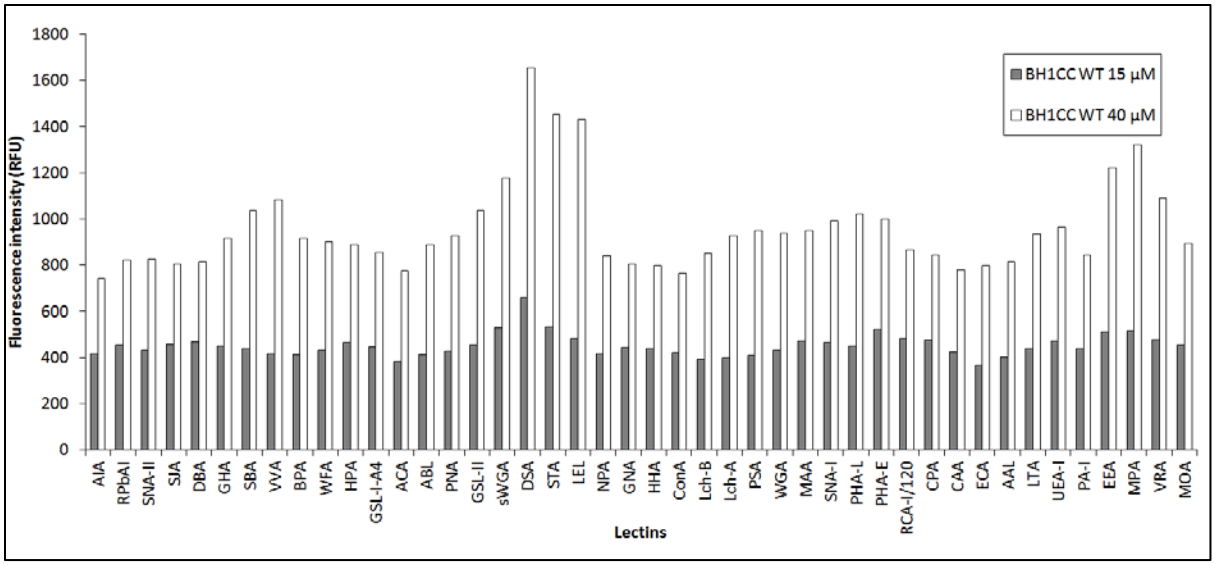

Figure S7. Lectin microarray background fluorescence of *S. aureus* BH1CC WT stained with 15 and 40 µM SYTO® 82. *S. aureus* BH1CC WT stained with 15 and 40 µM SYTO® 82 incubated on the lectin microarray and the local average background around each lectin represented as a bar chart. As 15 µM SYTO® 82 resulted in similar signal intensity with lower background compared to 40 µM, 15 µM was selected as the optimal concentration for staining *S. aureus* BH1CC WT and Δ*ica*.

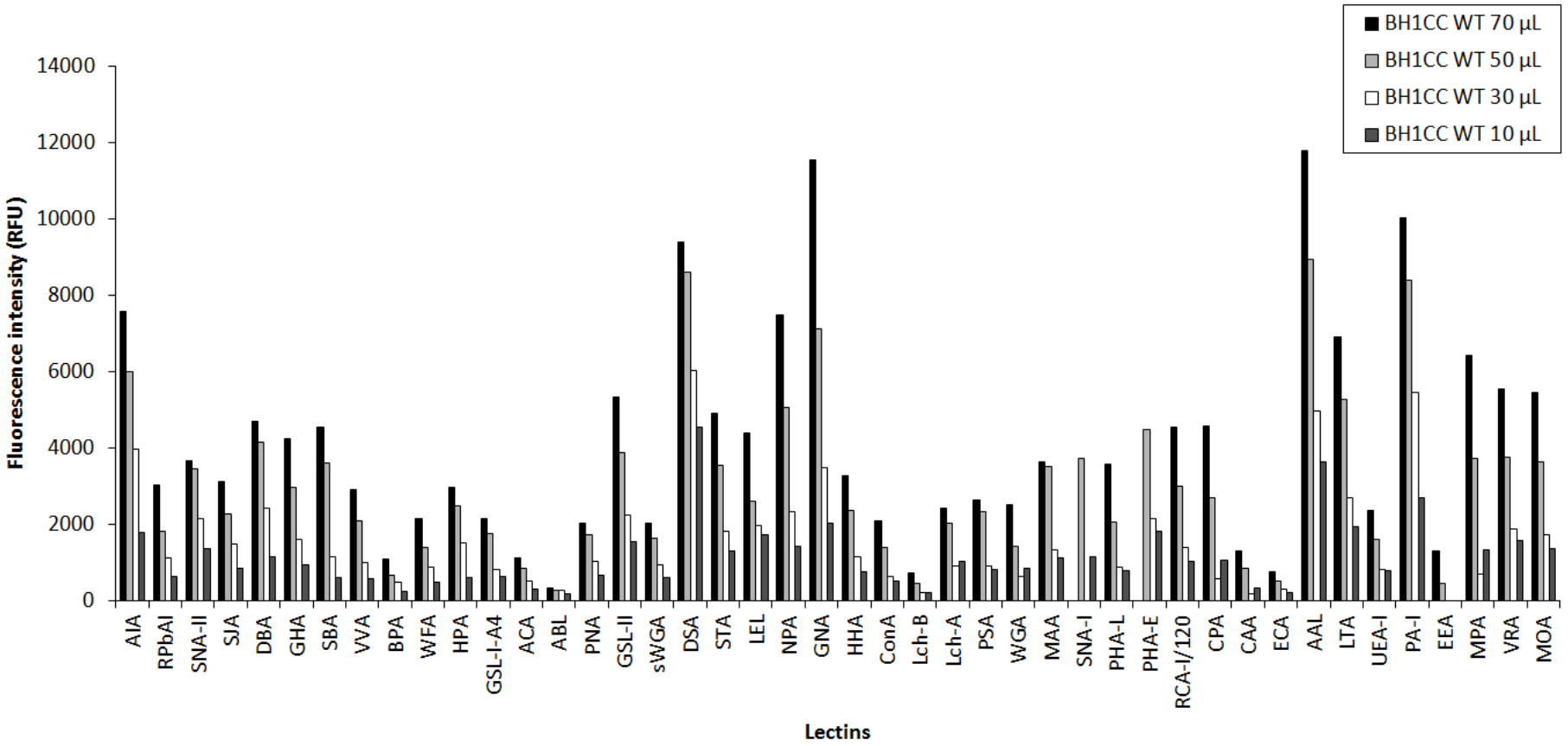

Figure S8. *S. aureus* BH1CC WT titration on the lectin microarray. *S. aureus* BH1CC was either not diluted (BH1CC WT 70 µL), 50 µL of the stained bacteria were diluted with TBS-T to a final volume of 70 µL (BH1CC WT 50 µL), 30 µL diluted to a final volume of 70 µL (BH1CC WT 30 µL) or 10 µL diluted to a final volume of 70 µL (BH1CC WT 10 µL) and incubated on the lectin microarray. Bars represent the binding intensity from one experiment and the median data from six technical replicates.

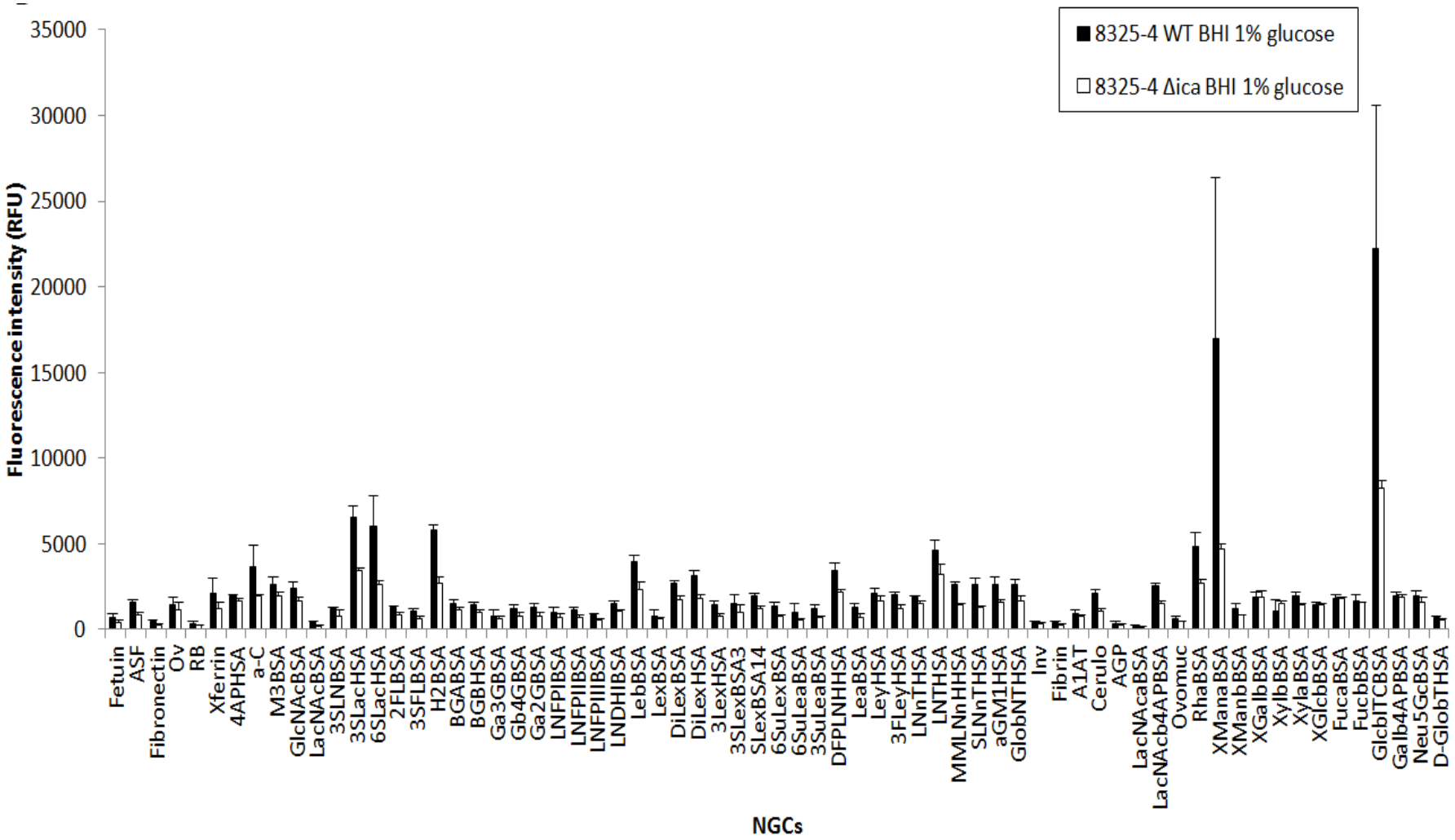

Figure S9. Carbohydrate microarray binding intensity profiles of *S. aureus* 8325-4 WT and Δ*ica* grown in BHI glucose. Bars represent the mean of three experiments with error bars of +/- 1 SD of the mean.

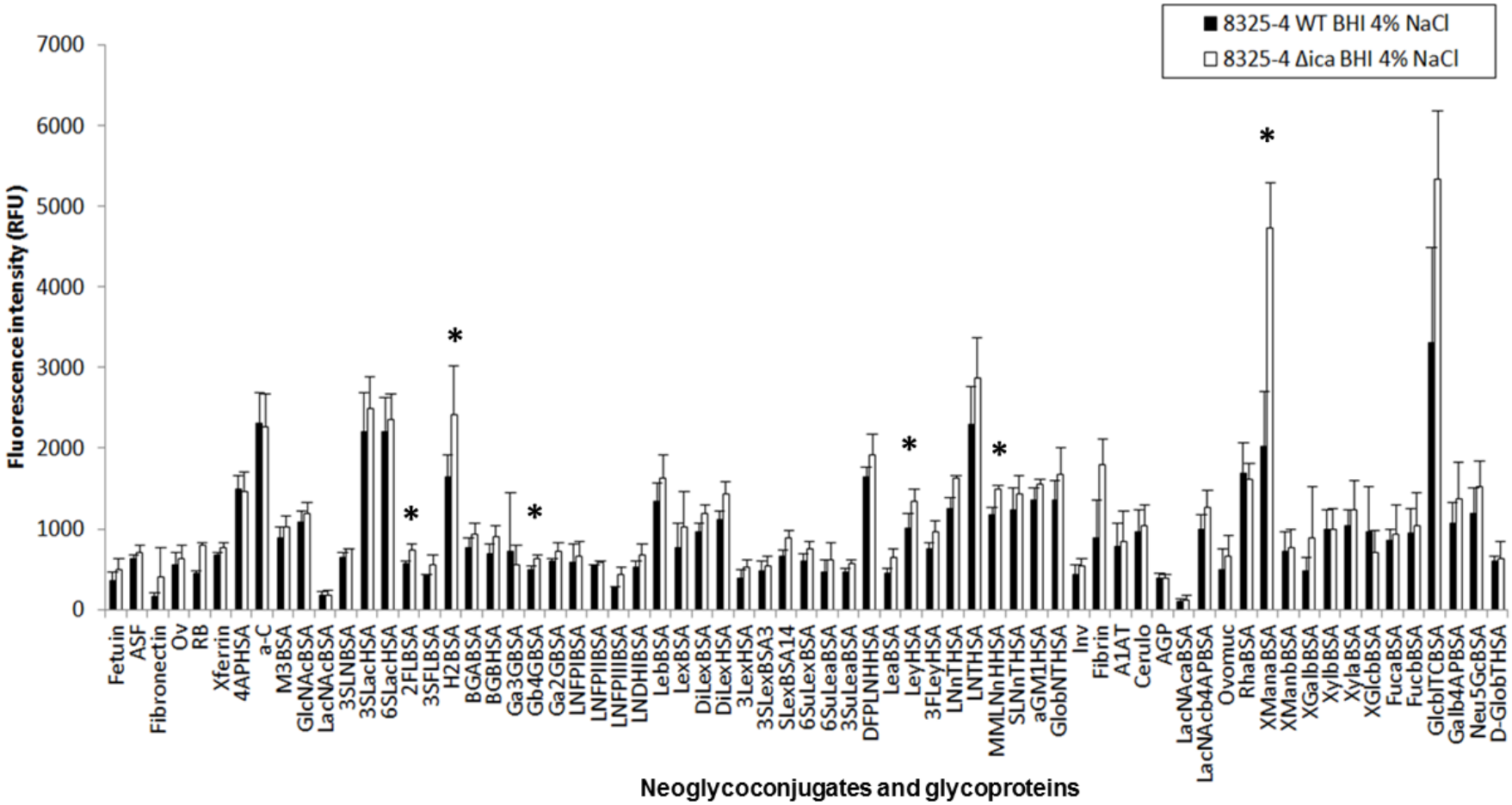

Figure S10. Carbohydrate microarray binding intensity profiles of *S. aureus* 8325-4 WT and Δ*ica* grown in BHI NaCl. Bars represent the mean of three experiments with error bars of +/- 1 SD of the mean. * represents significant difference ($p \leq 0.05$, calculated by student's t test, two tailed) in binding between WT and Δ*ica*.

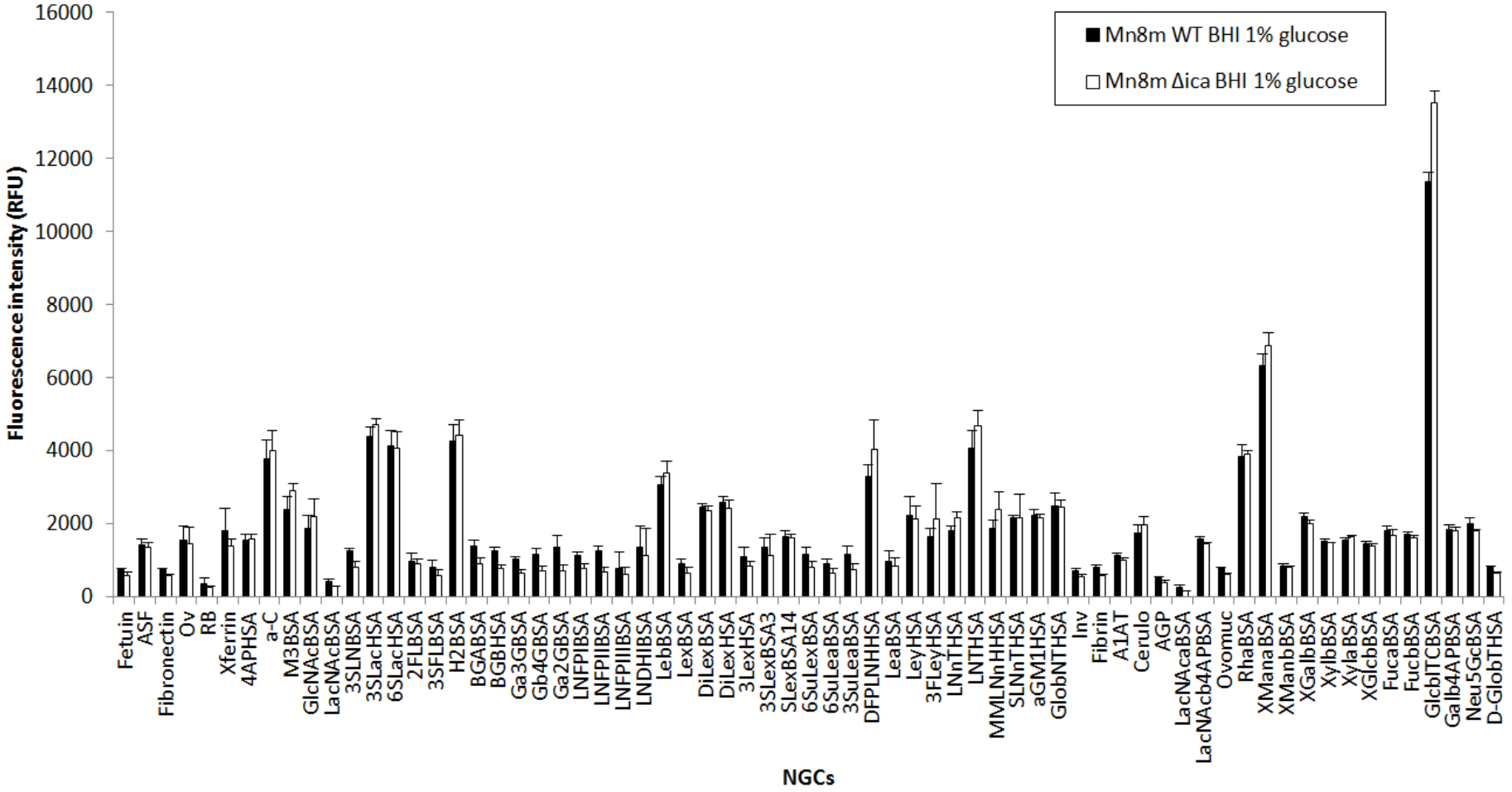

Figure S11. Carbohydrate microarray binding intensity profiles of *S. aureus* Mn8m WT and Δ*ica* grown in BHI glucose. Bars represent the mean of three experiments with error bars of +/- 1 SD of the mean.

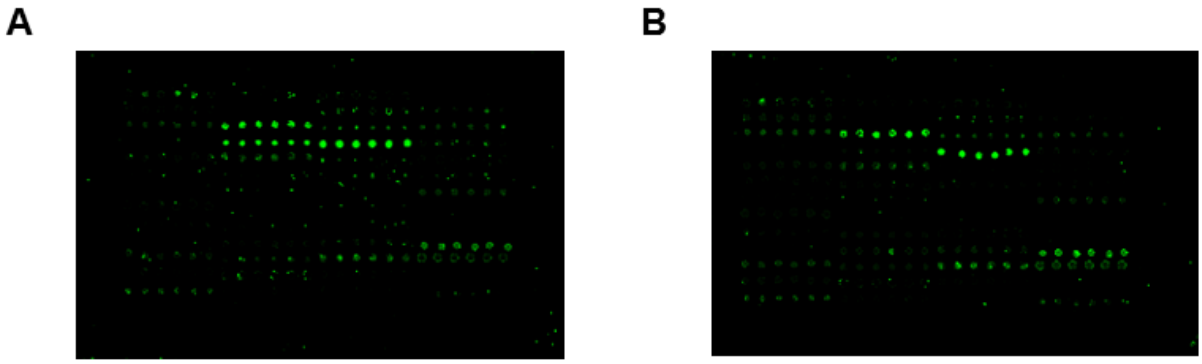

Figure S12. Example of lectin microarray subarrays incubated with fluorescently stained bacteria. (**A**) *S. aureus* Mn8m WT. (**B**) *S. aureus* Mn8m Δica mutant.

Tables

Table S1. The origins of bacterial strains used in this study.

Bacteria strains	**Details**	**Reference**
S. aureus 8325-4 WT	8325 derivative cured of prophages. 11-bp deletion in rsbU	[1]
S. aureus 8325-4 Δ*ica*	*icaADBC*::Tr^r isogenic mutant of 8325-4	[4]
S. aureus Mn8m WT	Chemostat derived mutant of Mn8 (toxic shock syndrome isolate). Biofilm positive.	[2]
S. aureus Mn8 Δ*ica*	*icaADBC*::Tr^r isogenic mutant of Mn8	[3]
S. aureus BH1CC WT	MRSA clinical isolate. Biofilm positive. SCCmec type, MLST type 8, clonal complex 8. Isolate from Beaumont Hospital, Dublin, Ireland.	[7]
S. aureus BH1CC Δ*ica*	*icaADBC*::Tr^r isogenic mutant of BH1CC	[4]
A. baumannii S1 WT	Clinical isolate. Mucoid phenotype. Biofilm positive.	[6]
A. baumannii S1 Δ*pga*	S1 derivative with in-frame deletion of *pgaABC*	[6]

Table S2. Lectins printed, their binding specificities, their simple print sugars (1 mM) and the supplying company. Binding specificity is reported recognition based on literature consensus or experimental evidence generated within our laboratory.

Abbreviation	Source	Species	Common name	General binding specificity	Print sugar	Supplier
AIA, Jacalin	Plant	*Artocarpus integrifolia*	Jack fruit lectin	Gal, Gal-β-(1,3)-GalNAc (sialylation independent)	Gal	EY Labs
RPbAI	Plant	*Robinia pseudoacacia*	Black locust lectin	Gal	Gal	EY Labs
SNA-II	Plant	*Sambucus nigra*	Sambucus lectin-II	Gal/GalNAc	Gal	EY Labs
SJA	Plant	*Sophora japonica*	Pagoda tree lectin	β-linked GalNAc	Gal	EY Labs
DBA	Plant	*Dolichos biflorus*	Horse gram lectin	GalNAc	Gal	EY Labs
GHA	Plant	*Glechoma hederacea*	Ground ivy lectin	GalNAc	Gal	EY Labs
SBA	Plant	*Glycine max*	Soy bean lectin	GalNAc	Gal	EY Labs
VVA	Plant	*Vicia villosa*	Hairy vetch lectin	GalNAc	Gal	EY Labs
BPA	Plant	*Bauhinia purpurea*	Camels foot tree lectin	GalNAc/Gal	Gal	EY Labs
WFA	Plant	*Wisteria floribunda*	Japanese wisteria lectin	GalNAc/sulfated GalNAc	Gal	EY Labs
HPA	Animal	*Helix pomatia*	Edible snail lectin	α-linked GalNAc	Gal	EY Labs
GSL-I-A4	Plant	*Griffonia simplicifolia*	Griffonia isolectin I A4	GalNac	Gal	EY Labs
ACA	Plant	*Amaranthus caudatus*	Amaranthin	Sialylated/Gal-β-(1,3)-GalNAc	Lac	Vector Labs
ABL	Fungus	*Agaricus bisporus*	Edible mushroom lectin	Gal-β(1,3)-GalNAc, GlcNAc	Lac	EY Labs
PNA	Plant	*Arachis hypogaea*	Peanut lectin	Gal-β-(1,3)-GalNAc	Lac	EY Labs
GSL-II	Plant	*Griffonia simplicifolia*	Griffonia lectin-II	GlcNAc	GlcNAc	EY Labs
sWGA	Plant	*Triticum vulgaris*	Succinyl WGA	GlcNAc	GlcNAc	EY Labs
DSA	Plant	*Datura stramonium*	Jimson weed lectin	GlcNAc	GlcNAc	EY Labs
STA	Plant	*Solanum tuberosum*	Potato lectin	GlcNAc oligomers	GlcNAc	EY Labs
LEL	Plant	*Lycopersicum eculentum*	Tomato lectin	GlcNAc-β-(1,4)-GlcNAc	GlcNAc	EY Labs
NPA	Plant	*Narcissus pseudonarcissus*	Daffodil lectin	α-(1,6)-Man	Man	EY Labs
GNA	Plant	*Galanthus nivalis*	Snowdrop lectin	Man-α-(1,3)-	Man	EY Labs
HHA	Plant	*Hippeastrum hybrid*	Amaryllis agglutinin	Man-α-(1,3)-Man-α-(1,6)-	Man	EY Labs
ConA	Plant	*Canavalia ensiformis*	Jack bean lectin	Man, Glc, GlcNAc	Man	EY Labs
Lch-B	Plant	*Lens culinaris*	Lentil isolectin B	Man, core fucosylated, agalactosylated biantennary *N*-glycans	Man	EY Labs
Lch-A	Plant	*Lens culinaris*	Lentil isolectin A	Man/Glc	Man	EY Labs

PSA	Plant	*Pisum sativum*	Pea lectin	Man, core fucosylated trimannosyl *N*-glycans	Man	EY Labs
TJA-I	Plant	*Trichosanthes japonica*	Trichosanthes japonica agglutinin I	NeuAc-α-(2,6)-Gal-β-(1,4)-GIcNAc	Lac	Medicago
WGA	Plant	*Triticum vulgaris*	Wheat germ agglutinin	NeuAc/GlcNAc	GlcNAc	EY Labs
MAA	Plant	*Maackia amurensis*	Maackia agglutinin	Sialic acid-α-(2,3)-linked	Lac	EY Labs
SNA-I	Plant	*Sambucus nigra*	Sambucus lectin-I	Sialic acid-α-(2,6)-linked	Lac	EY Labs
PHA-L	Plant	*Phaseolus vulgaris*	Kidney bean leukoagglutinin	Tri- and tetraantennary β-Gal/Gal-β-(1,4)-GlcNAc	Lac	EY Labs
PHA-E	Plant	*Phaseolus vulgaris*	Kidney bean erythroagglutinin	Biantennary with bisecting GlcNAc,β-Gal/Gal-β-(1,4)-GlcNAc	Lac	EY Labs
RCA-I/120	Plant	*Ricinus communis*	Castor bean lectin I	Gal-β-(1,4)-GlcNAc	Gal	Vector Labs
AMA	Plant	*Arum maculatum*	Lords and ladies lectin	Gal-β-(1,4)-GlcNAc	Lac	EY Labs
CPA	Plant	*Cicer arietinum*	Chickpea lectin	Complex oligosaccharides	Lac	EY Labs
CAA	Plant	*Caragana arborescens*	Pea tree lectin	Gal-β-(1,4)-GlcNAc	Lac	EY Labs
ECA	Plant	*Erythrina cristagalli*	Cocks comb/coral tree lectin	Gal-β-(1,4)-GlcNAc oligomers	Lac	EY Labs
TJA-II	Plant	*Trichosanthes japonica*	Trichosanthes japonica agglutinin II	Fuc-α-(1,2)-Gal-β-(1,4)-GlcNAc	Lac	Medicago
AAL	Fungi	*Aleuria aurantia*	Orange peel fungus lectin	Fuc-α-(1,6)-linked, Fuc-α-(1,3)-linked	Fuc	Vector Labs
LTA	Plant	*Lotus tetragonolobus*	Lotus lectin	Fuc-α-(1,3)-linked	Fuc	EY Labs
UEA-I	Plant	*Ulex europaeus*	Gorse lectin-I	Fuc-α-(1,2)-Gal	Fuc	EY Labs
PA-I	Bacteria	*Pseudomonas aeruginosa*	Pseudomonas lectin	Terminal α-linked Gal, Gal derivatives	Gal	EY Labs
EEA	Plant	*Euonymous europaeus*	Spindle tree lectin	Terminal α-linked Gal	Gal	EY Labs
MPA	Plant	*Maclura pomifera*	Osage orange lectin	Terminal α-linked Gal	Gal	EY Labs
VRA	Plant	*Vigna radiata*	Mung bean lectin	Terminal α-linked Gal	Gal	EY Labs
MOA	Fungus	*Marasmius oreades*	Fairy ring mushroom lectin	Terminal α-linked Gal	Gal	EY Labs

Table S3. Print list for carbohydrate microarray A and source of printed probes. All probes were printed at 1 mg/mL. Common probes for normalisation between microarrays A and B are shaded in blue below. Substitution measurement method indicated by M, MALDI; T, ToF MS; C, colourimetric assay. In house stocks synthesised as previously described [12].

Abbreviation	Probe	Source	Cat. No.	Spacer length	Structure	Substitution Average	Substitution Range
Fetuin	Fetuin from fetal bovine serum	Sigma	F2379		Glycoprotein		
ASF	Asialofetuin	Sigma			Desialylated glycoprotein		
Fibronectin	Fibronectin	Collaborative Research Inc.			Glycoprotein		
Ov	Ovalbumin from chicken egg white, grade VI	Sigma	A2512		Phosphorylated glycoprotein		
RB	RNAse B	Sigma			Glycoprotein		
Xferrin	Transferrin	Sigma			Glycoprotein		
4APHSA	4AP-HSA	In house			4AP-HSA		
α-C	α-Crystallin from bovine lens	Sigma	C4163		Phosphorylated glycoprotein		
M3BSA	Man α1,3(Man α1,6)Man-BSA	Dextra	NGP1336		Man-α-(1,3)-[Man-α-(1,6)-]Man-BSA	23 (T)	9 to 35
GlcNAcBSA	GlcNAc-BSA	Dextra	NGP1101	14 atom	GlcNAc-Sp14-NH2(Lys)-BSA	39 (T)	28 to 48
LacNAcBSA	LacNAc-BSA	Dextra	NGP0201		Gal-β-(1,4)-GlcNAc-Sp3-BSA	11 (M)	8 to 15
3SLNBSA	3'SialylLacNAc-BSA	Dextra	NGP0301	3 atom	Neu5Ac-α-(2,3)-Gal-β-(1,4)-GlcNAc-Sp3-BSA	13 (M)	8 to 25
3SLacHSA	3´-Sialyllactose-APD-HSA,	IsoSep	60/67		Neu5Ac-α-(2,3)-Gal-β-(1,4)-(Glc)-APD-HSA	6 (T)	
6SLacHSA	6´-Sialyllactose-APD-HSA,	IsoSep	60/93		Neu5Ac-α-(2,6)-Gal-β-(1,4)-(Glc)-APD-HSA	15 (T)	
2FLBSA	2'Fucosyllactose-BSA	Dextra	NGP0307		Fuc-α-(1,2)-Gal-β-(1,4)-Glc-Sp3-BSA	7 (M)	4 to 10
3SFLBSA	3'Sialyl-3-fucosyllactose-BSA	Dextra	NGP0405		Neu5Ac-α-(2,3)-Gal-β-(1,4)-[Fuc-α-(1,3)-]Glc-Sp3-BSA	7 (M)	5 to 10
H2BSA	H Type II-APE-BSA	IsoSep	60/54		Fuc-α-(1,2)-Gal-β-(1,4)-GlcNAc-β-(1-APE-BSA	26	
BGABSA	Blood Group A-BSA	Dextra	NGP6305	6 atom	GalNAc-α-(1,3)-[Fuc-α-(1,2)-]Gal-BSA	19 (M)	11 to 28
BGBHSA	Blood Group B-HSA	Dextra	NGP9323	6 atom	Gal-α-(1,3)-[Fuc-α-(1,2)-]Gal-BSA	21 (M)	

Ga3GBSA	Galα1,3Gal-BSA	Dextra	NGP0203		Gal-α-(1,3)-Gal-Sp3-BSA	20 (M)	15 to 26
Gb4GBSA	Galb1,4GalBSA	Dextra	NGP0204		Gal-β-(1,4)-Gal-Sp3-BSA	16 (M)	9 to 29
Ga2GBSA	Gala1,2GalBSA	Dextra	NGP0202		Gal-α-(1,2)-Gal-Sp3-BSA	12 (M)	5 to 21
LNFPIBSA	Lacto-*N*-fucopentaose I-BSA	Dextra	NGP0503		Fuc-α-(1,2)-Gal-β-(1,3)-GlcNAc-β-(1,3)-Gal-β-(1,4)-Glc-BSA	20 (M)	11 to 30
LNFPIIBSA	Lacto-*N*-fucopentaose II-BSA	Dextra	NGP0501		Fuc-α-(1,3)-Gal-β-(1,3)-GlcNAc-β-(1,3)-Gal-β-(1,4)-Glc-BSA	15 (M)	6 to 31
LNFPIIIBSA	Lacto-*N*-fucopentaose III-BSA	Dextra	NGP0502		Gal-β-(1,4)-[Fuc-α-(1,3)-]GlcNAc-β-(1,3)-Gal-β-(1,4)-Glc-BSA	20 (M)	12 to 29
LNDHIBSA	Lacto-*N*-difucohexaose I-BSA	Dextra	NGP0601		Fuc-α-(1,2)-Gal-β-(1,3)-[Fuc-α-(1,4)-]GlcNAc-β-(1,3)-Gal-β-(1,4)-(Glc)-Sp3-BSA	7.5 (T)	4 to 12
LebBSA	LNDI-BSA/ Lewis b-BSA	IsoSep	60/04		Fuc-α-(1,2)-Gal-β-(1,3)-[Fuc-α-(1,4)-]GlcNAc-β-(1,3)-Gal-β-(1,4)-(Glc)-APD-BSA	10	
LexBSA	Lewis x-BSA	Dextra	NGP0302		Gal-β-(1,4)-[Fuc-α-(1,3)-]GlcNAc-BSA	24 (M)	13 to 35
DiLexBSA	Di-Lex-APE-BSA	IsoSep	61/64		Gal-β-(1,4)-[Fuc-α-(1,3)-]GlcNAc-β-(1,3)-Gal-β-(1,4)-[Fuc-α-(1,3)-]GlcNAc-β-(1-O-APE-BSA	28 (C)	
DiLexHSA	Di-Lewisx-APE-HSA	IsoSep	61/59		Gal-β-(1,4)-[Fuc-α-(1,3)-]GlcNAc-β-(1,3)-Gal-β-(1,4)-[Fuc-α-(1,3)-]GlcNAc-β-(1-O-APE-HSA	18 (T)	
3LexHSA	Tri-Lex-APE-HSA	IsoSep	61/56		Gal-β-(1,4)-[Fuc-α-(1,3)-]GlcNAc-β-(1,3)-Gal-β-(1,4)-[Fuc-α-(1,3)-]GlcNAc−β-(1,3)-Gal-β-(1,4)-[Fuc-α-(1,3)-]GlcNAc-β-(1-O-APE-HSA	15 (T)	
3SLexBSA3	3'Sialyl Lewis x-BSA	Dextra	NGP0403	3 atom	Neu5Ac-α-(2,3)-Gal-β-(1,4)-[Fuc-α-(1,3)-]GlcNAc-Sp3-BSA	9 (M)	3 to 16
SLexBSA14	3'Sialyl Lewis x-BSA	Dextra	NGP1403	14 atom	Neu5Ac-α-(2,3)-Gal-β-(1,4)-[Fuc-α-(1,3)-]GlcNAc-Sp14-BSA	8 (T)	6 to 15
6SuLexBSA	6-Sulfo Lewis x-BSA	Dextra	NGP0603		(SO_4)6Gal-β-(1,4)-[Fuc-α-(1,3)-]GlcNAc-Sp3-BSA	8 (M)	1 to 16
6SuLeaBSA	6-Sulfo Lewis a-BSA	Dextra	NGP0604		(SO_4)6Gal-β-(1,3)-[Fuc-α-(1,4)-]GlcNAc-Sp3-BSA	17 (M)	8 to 28
3SuLeaBSA	3-Sulfo Lewis a-BSA	Dextra	NGP0304		(SO_4)3Gal-β-(1,3)-[Fuc-α-(1,4)-]GlcNAc-Sp3-BSA	15 (M)	9 to 20
PBS	PBS						
DFPLNHHSA	Difucosyl-para-lacto-N-hexaose-APD-HSA, (Lea/Lex)	IsoSep	61/57		Gal-β-(1,3)-[Fuc-α-(1,4)-]GlcNAc-β-(1,3)-Gal-β-(1,4)-[Fuc-α-(1,3)-]GlcNAc-β-(1,3)-Gal-β-(1,4)-(Glc)-APD-HSA	21 (T)	

LeaBSA	Lewis a-BSA	Dextra	NGP0704		Gal-β-(1,3)-[Fuc-α-(1,4)-]GlcNAc-Sp3-BSA	12 (M)	2 to 28
LeyHSA	Lewis y-tetrasaccharide-APE-HSA	IsoSep	60/95		Fuc-α-(1,2)-Gal-β-(1,4)-[Fuc-α-(1,3)-]GlcNAc-β-(1-O-APE-HSA	13.3 (T)	
3FLeyHSA	Tri-fucosyl-Ley-heptasaccharide-APE-HSA	IsoSep	61/63		Fuc-α-(1,2)-Gal-β-(1,4)-[Fuc-α-(1,3)-]GlcNAc-β-(1,3)-Gal-β-(1,4)-[Fuc-α-(1,3)-]GlcNAc-β-(1-O-APE-HSA	11 (T)	
LNnTHSA	Lacto-N-neotetraose-APD-HSA	IsoSep	60/72		Gal-β-(1,4)-GlcNAc-β-(1,3)-Gal-β-(1,4)-(Glc)-APD-HSA	9.2 (M)	
LNTHSA	Lacto-N-tetraose-APD-HSA	IsoSep	60/97		Gal-β-(1,3)-GlcNAc-β-(1,3)-Gal-β-(1,4)-(Glc)-APD-HSA	22 (T)	
MMLNnHHSA	Monofucosyl, monosialyllacto-N-neohexaose-APD-HSA	IsoSep	61/62		Neu5Ac-α-(2,3)-Gal-β-(1,4)-GlcNAc-β-(1,3)-[Gal-β-(1,4)-[Fuc-α-(1,3)-]GlcNAc-β-(1,6)-]Gal-β-(1,4)-(Glc)-APD-HSA	15 (T)	
SLNnTHSA	Sialyl-LNnT-penta-APD-HSA	IsoSep	61/68		Neu5Ac-α-(2,3)-Gal-β-(1,4)-GlcNAc-β-(1,3)-Gal-β-(1,4)-(Glc)-APD-HSA	9.3 (T)	
aGM1HSA	Asialo-GM1-tetrasaccharide-APD-HSA	IsoSep	60/96		Gal-β-(1,3)-GalNAc-β-(1,4)-Gal-β-(1,4)-(Glc)-APD-HSA	10 ©	
GlobNTHSA	Globo-N-tetraose-APD-HSA	IsoSep	60/99		GalNAc-β-(1,3)-Gal-α-(1,4)-Gal-β-(1,4)-(Glc)-APD-HSA	8.4 (T)	
GlobTHSA	Globotriose-APD-HSA	IsoSep	60/90		Gal-α-(1,4)-Gal-β-(1,4)-Glc-β-(1-APE-HSA	21 (T)	

Table S4. Print list for carbohydrate microarray B and source of printed probes. All probes were printed at 1 mg/mL except fibrinogen (fibrin), ovomucoid (ovomuc) and Tri-Lex-APE-HSA (3LexHSA) were printed at 0.5 mg/mL. Common probes for normalisation between microarrays A and B are shaded in blue below. Substitution measurement method indicated by M, MALDI; T, ToF MS; C, colourimetric assay. In house stocks synthesised as previously described [12].

Abbreviation	**Neoglycoconjugate**	**Source**	**Cat. No.**	**Spacer length**	**Structure**	**Substitution Average**	**Substitution Range**
Fetuin	Fetuin from fetal bovine serum	Sigma	F2379		Glycoprotein		
Inv	Invertase, grade VII	Sigma	I4504		Glycoprotein		

Fibrin	Fibrinogen	Sigma	F-4129		Glycoprotein		
Ov	Ovalbumin from chicken egg white, grade VI	Sigma	A2512		Phosphorylated glycoprotein		
PBS	PBS						
A1AT	alpha-1-antitrypsin	Sigma	A-6388		Glycoprotein		
4APHSA	4AP-HSA	In house			4AP-HSA		
α -C	α-Crystallin from bovine lens	Sigma	C4163		Phosphorylated glycoprotein		
M3BSA	Manα1,3(Manα1,6)Man-BSA	Dextra	NGP1336		Man-α-(1,3)-[Man-α-(1,6)-]Man-BSA	23 (T)	9 to 35
GlcNAcBSA	GlcNAc-BSA	Dextra	NGP1101	14 atom	GlcNAc-Sp14-NH2(Lys)-BSA	39 (T)	28 to 48
Cerulo	Ceruloplasmin, human, type III	Sigma	C-3007		Glycoprotein	11 (M)	8 to 15
AGP	alpha-1-acid glycoprotein, human	Sigma	G9885		Glycoprotein	13 (M)	8 to 25
3SLacHSA	3´-Sialyllactose-APD-HSA	IsoSep	60/67		Neu5Ac-α-(2,3)-Gal-β-(1,4)-(Glc)-APD-HSA	6 (T)	
6SLacHSA	6´-Sialyllactose-APD-HSA	IsoSep	60/93		Neu5Ac-α-(2,6)-Gal-β-(1,4)-(Glc)-APD-HSA	15 (T)	
LacNAcaBSA	LacNAc-α-4AP-BSA	In house			LacNAc-α-4AP-BSA		
LacNAcb4APBSA	LacNAc-β-4AP-BSA	In house			LacNAc-β-4AP-BSA		
H2BSA	H Type II-APE-BSA	IsoSep	60/54		Fuc-α-(1,2)-Gal-β-(1,4)-GlcNAc-β-(1-APE-BSA	26	
PBS	PBS						
Ovomuc	Ovomucoid	Dextra	T-9253		Glycoprotein		
Ga3GBSA	Galα1,3Gal-BSA	Dextra	NGP0203	3 at om	Gal-α-(1,3)-Gal-Sp3-BSA	20 (M)	15 to 26
RhaBSA	L-Rhamnose-BSA	Dextra	NGP1106	14 atom	L-Rhamnose-Sp14-BSA	32 (M)	16 to 54
PBS	PBS						
LNFPIBSA	Lacto-*N*-fucopentaose I-BSA	Dextra	NGP0503		Fuc-α-(1,2)-Gal-β-(1,3)-GlcNAc-β-(1,3)-Gal-β-(1,4)-Glc-BSA	20 (M)	11 to 30
XManaBSA	Man-α-ITC-BSA	In house			Man-α-ITC-BSA		
PBS	PBS	Dextra					
XManbBSA	Man-β-4AP-BSA	In house			Man-β-4AP-BSA		

LebBSA	LNDI-BSA/ Lewis b-BSA	IsoSep	60/04		Fuc-α-(1,2)-Gal-β-(1,3)-[Fuc-α-(1,4)-]GlcNAc-β-(1,3)-Gal-β-(1,4)-(Glc)-APD-BSA	10	
LexBSA	Lewis x-BSA	Dextra	NGP0302		Gal-β-(1,4)-[Fuc-α-(1,3)-]GlcNAc-BSA	24 (M)	13 to 35
XGalbBSA	Gal-β-ITC-BSA	In house					
XylbBSA	Xyl-β-4AP-BSA	In house					
3LexHSA	Tri-Lex-APE-HSA	IsoSep	61/56		Gal-β-(1,4)-[Fuc-α-(1,3)-]GlcNAc-β-(1,3)-Gal-β-(1,4)-[Fuc-α-(1,3)-]GlcNAc−β-(1,3)-Gal-β-(1,4)-[Fuc-α-(1,3)-]GlcNAc-β-(1-O-APE-HSA	15 (T)	
XylaBSA	Xyl-α-4AP-BSA	In house			Xyl-α-4AP-BSA		
XGlcbBSA	Glc-β-4AP-BSA	In house			Glc-β-4AP-BSA		
FucaBSA	Fuc-α-4AP-BSA	In house			Fuc-α-4AP-BSA		
6SuLeaBSA	6-Sulfo Lewis a-BSA	Dextra	NGP0604	3 atom	(SO_4)6Gal-β-(1,3)-[Fuc-α-(1,4)-]GlcNAc-Sp3-BSA	17 (M)	8 to 28
FucbBSA	Fuc-β-4AP-BSA	In house			Fuc-β-4AP-BSA		
GlcbITCBSA	Glc-β-ITC-BSA	In house			Glc-β-ITC-BSA		
Galb4APBSA	Gal-β-4AP-BSA	In house			Gal-β-4AP-BSA		
Neu5GcBSA	Neu5Gc-BSA	In house			Neu5Gc-BSA		
LeyHSA	Lewis y-tetrasaccharide-APE-HSA	IsoSep	60/95		Fuc-α-(1,2)-Gal-β-(1,4)-[Fuc-α-(1,3)-]GlcNAc-β-(1-O-APE-HSA	13.3 (T)	
PBS							
PBS							
LNTHSA	Lacto-N-tetraose-APD-HSA	IsoSep	60/97		Gal-β-(1,3)-GlcNAc-β-(1,3)-Gal-β-(1,4)-(Glc)-APD-HSA	22 (T)	
PBS							
PBS							
D-GlobTHSA	Globotriose-HSA	Dextra	NGP2340	3 atom	Gal-α-(1,4)-Gal-β-(1,4)-Glc-Sp3-BSA	12.7 (M)	8 to 19
GlobNTHSA	Globo-N-tetraose-APD-HSA	IsoSep	60/99		GalNAc-β-(1,3)-Gal-α-(1,4)-Gal-β-(1,4)-(Glc)-APD-HSA	8.4 (T)	
GlobTHSA	Globotriose-APE-HSA	IsoSep	60/90		Gal-α-(1,4)-Gal-β-(1,4)-Glc-β-(1-APE-HSA	21 (T)	

MATERIALS AND METHODS

Assay for retained PNAG after washing. Cultures were grown overnight in BHI NaCl, washed three times in TBS and cells were adjusted to an absorbance of approximately 1.0 at 595 nm. Bacteria cultures were placed in to tubes in 1 mL aliquots to act as a positive control and were set aside. Separate 1 mL cultures were washed one to five times by resuspending in TBS, centrifuging the bacteria in to a pellet at 5,000 x g and removing the supernatant each time. After the final wash, bacterial pellets were resuspended in 1 mL TBS or TBS with 0.05%, 0.02% or 0.01% (v/v) Tween® 20. Washed and unwashed 1 mL bacterial suspensions were collected by centrifugation (5,000 × g for 5 min), resuspended in 250 µL of 0.5 M ethylenediaminetetraacetic acid (EDTA) and boiled for 5 min. Samples were centrifuged and 40 µL aliquots of the supernatant were treated with proteinase K (10 µL of 20 µg/mL) at 65 ^{o}C for 1 h and then boiled again for 5 min. The proteinase K-treated samples (2 µL) were pipetted on to a PVDF membrane in triplicate and the membrane was blocked and probed for PNAG using anti-PNAG IgG1 mAb as described above. After imaging HRP activity on the membrane, digital images (.jpg) were saved and used to relatively quantify the amounts of PNAG present on the membrane compared to the control (PNAG without three washes) using ImageJ software (National Institutes of Health, Bethesda, MD, U.S.A.). Measurements using the same size frame were taken for each spot, the frames were analysed and the resulting data was exported into Excel v.2010 (Microsoft). The mean of technical triplicates was taken for each condition and expressed as a percentage of intensity of unwashed cells.

References

1. Horsburgh, M.J.; Aish, J.L.; White, I.J.; Shaw, L.; Lithgow, J.K.; Foster, S.J. Σ^{b} modulates virulence determinant expression and stress resistance: Characterization of a functional *rsbu* strain derived from *Staphylococcus aureus* 8325-4. *J. Bacteriol.* **2002**, *184*, 5457-5467.
2. McKenney, D.; Pouliot, K.L.; Wang, Y.; Murthy, V.; Ulrich, M.; Döring, G.; Lee, J.C.; Goldmann, D.A.; Pier, G.B. Broadly protective vaccine for *Staphylococcus aureus* based on an *in vivo*-expressed antigen. *Science* **1999**, *284*, 1523-1527.
3. Jefferson, K.K.; Cramton, S.E.; Götz, F.; Pier, G.B. Identification of a 5-nucleotide sequence that controls expression of the ica locus in *staphylococcus aureus* and characterization of the DNA-binding properties of icar. *Mol. Microbiol.* **2003**, *48*, 889-899.
4. Fitzpatrick, F.; Humphreys, H.; O'Gara, J.P. Evidence for *icaadbc*-independent biofilm development mechanism in methicillin-resistant *Staphylococcus aureus* clinical isolates. *J. Clin. Microbiol.* **2005**, *43*, 1973-1976.

5. Houston, P.; Rowe, S.E.; Pozzi, C.; Waters, E.M.; O'Gara, J.P. Essential role for the major autolysin in the fibronectin-binding protein-mediated *Staphylococcus aureus* biofilm phenotype. *Infect. Immun.* **2011**, *79*, 1153-1165.
6. Choi, A.H.K.; Slamti, L.; Avci, F.Y.; Pier, G.B.; Maira-Litrán, T. The *pgaabcd* locus of *Acinetobacter baumannii* encodes the production of poly-β-1-6-*N*-acetylglucosamine, which is critical for biofilm formation. *J. Bacteriol.* **2009**, *191*, 5953-5963.
7. O'Neill, E.; Pozzi, C.; Houston, P.; Smyth, D.; Humphreys, H.; Robinson, D.A.; O'Gara, J.P. Association between methicillin susceptibility and biofilm regulation in *Staphylococcus aureus* isolates from device-related infections. *J. Clin. Microbiol.* **2007**, *45*, 1379-1388.
8. O'Neill, E.; Pozzi, C.; Houston, P.; Humphreys, H.; Robinson, D.A.; Loughman, A.; Foster, T.J.; O'Gara, J.P. A novel *Staphylococcus aureus* biofilm phenotype mediated by the fibronectin-binding proteins, Fnbpa and Fnbpb. *J. Bacteriol.* **2008**, *190*, 3835-3850.
9. Kennedy, C.A.; O' Gara, J.P. Contribution of culture media and chemical properties of polystyrene tissue culture plates to biofilm development by *Staphylococcus aureus*. *J. Med. Microbiol.* **2004**, *53*, 1171-1173.
10. Kilcoyne, M.; Twomey, M.E.; Gerlach, J.Q.; Kane, M.; Moran, A.P.; Joshi, L. *Campylobacter jejuni* strain discrimination and temperature-dependent glycome expression profiling by lectin microarray. *Carbohydr. Res.* **2014**, *389*, 123-133.
11. Maira-Litrán, T.; Kropec, A.; Abeygunawardana, C.; Joyce, J.; Mark, G.; Goldmann, D.A.; Pier, G.B. Immunochemical properties of the staphylococcal poly-*N*-acetylglucosamine surface polysaccharide. *Infect. Immun.* **2002**, *70*, 4433-4440.
12. Kilcoyne, M.; Gerlach, J.Q.; Kane, M.; Joshi, L. Surface chemistry and linker effects on lectin–carbohydrate recognition for glycan microarrays. *Anal. Methods* **2012**, *4*, 2721-2728.